


# 100 years of Brillouin scattering: Historical and future perspectives

Cite as: Appl. Phys. Rev. **9**, 041306 (2022); <https://doi.org/10.1063/5.0095488>

Submitted: 11 April 2022 • Accepted: 14 September 2022 • Published Online: 10 November 2022

 Moritz Merklein,  Irina V. Kabakova, Atiyeh Zarifi, et al.

## COLLECTIONS

 This paper was selected as Featured



View Online



Export Citation



CrossMark

## ARTICLES YOU MAY BE INTERESTED IN

[Atomic layer deposition of conductive and semiconductive oxides](#)




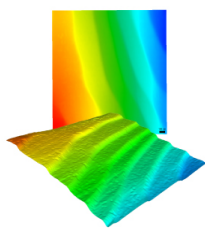
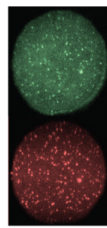
Applied Physics Reviews **9**, 041313 (2022); <https://doi.org/10.1063/5.0116732>

[Sustainable carbon sources for green laser-induced graphene: A perspective on fundamental principles, applications, and challenges](#)

Applied Physics Reviews **9**, 041305 (2022); <https://doi.org/10.1063/5.0100785>

[Advanced thermal sensing techniques for characterizing the physical properties of skin](#)

Applied Physics Reviews **9**, 041307 (2022); <https://doi.org/10.1063/5.0095157>

 <b>MCL</b> MAD CITY LABS INC. <a href="http://www.madcitylabs.com">www.madcitylabs.com</a>	<p>Nanopositioning Systems</p> 	<p>Modular Motion Control</p> 	<p>AFM and NSOM Instruments</p> 	<p>Single Molecule Microscopes</p> 
---	--	--	---	--

# 100 years of Brillouin scattering: Historical and future perspectives

Cite as: Appl. Phys. Rev. **9**, 041306 (2022); doi: [10.1063/5.0095488](https://doi.org/10.1063/5.0095488)

Submitted: 11 April 2022 · Accepted: 14 September 2022 ·

Published Online: 10 November 2022



View Online



Export Citation



CrossMark

Moritz Merklein,<sup>1,2,a)</sup>  Irina V. Kabakova,<sup>3,b)</sup>  Atiyeh Zarifi,<sup>1,2</sup> and Benjamin J. Eggleton<sup>1,2,c)</sup> 

## AFFILIATIONS

<sup>1</sup>The University of Sydney Nano Institute (Sydney Nano), The University of Sydney, New South Wales 2006, Australia

<sup>2</sup>Institute of Photonics and Optical Science (IPOS), School of Physics, The University of Sydney, New South Wales 2006, Australia

<sup>3</sup>School of Mathematical and Physical Sciences, University of Technology Sydney, New South Wales 2007, Australia

<sup>a)</sup>Electronic address: [moritz.merklein@sydney.edu.au](mailto:moritz.merklein@sydney.edu.au)

<sup>b)</sup>Electronic address: [irina.kabakova@uts.edu.au](mailto:irina.kabakova@uts.edu.au)

<sup>c)</sup>Author to whom correspondence should be addressed: [benjamin.eggleton@sydney.edu.au](mailto:benjamin.eggleton@sydney.edu.au)

## ABSTRACT

The Year 2022 marks 100 years since Leon Brillouin predicted and theoretically described the interaction of optical waves with acoustic waves in a medium. Accordingly, this resonant multi-wave interaction is referred to as Brillouin scattering. Today, Brillouin scattering has found a multitude of applications, ranging from microscopy of biological tissue, remote sensing over many kilometers, and signal processing in compact photonic integrated circuits smaller than the size of a thumbnail. What allows Brillouin scattering to be harnessed over such different length scales and research domains are its unique underlying properties, namely, its narrow linewidth in the MHz range, a frequency shift in the GHz range, large frequency selective gain or loss, frequency tunability, and optical reconfigurability. Brillouin scattering is also a ubiquitous effect that can be observed in many different media, such as freely propagating in gases and liquids, as well as over long lengths of low-loss optical glass fibers or short semiconductor waveguides. A recent trend of Brillouin research focuses on micro-structured waveguides and integrated photonic platforms. The reduction in the size of waveguides allows tailoring the overlap between the optical and acoustic waves and promises many novel applications in a compact footprint. In this review article, we give an overview of the evolution and development of the field of Brillouin scattering over the last one hundred years toward current lines of active research. We provide the reader with a perspective of recent trends and challenges that demand further research efforts and give an outlook toward the future of this exciting and diverse research field.

© 2022 Author(s). All article content, except where otherwise noted, is licensed under a Creative Commons Attribution (CC BY) license (<http://creativecommons.org/licenses/by/4.0/>). <https://doi.org/10.1063/5.0095488>

## TABLE OF CONTENTS

I. INTRODUCTION AND OUTLINE . . . . .	2	B. Distributed sensing using backward Brillouin scattering . . . . .	8
II. HISTORICAL DEVELOPMENT OF DIFFERENT PLATFORMS . . . . .	2	C. Distributed sensing using forward Brillouin scattering . . . . .	10
III. BRILLOUIN SCATTERING IN GASES, CRYSTALS, LIQUIDS, AND BIOLOGICAL MATERIALS. . . . .	3	V. MICROMETER-SCALE WAVEGUIDES AND CHIP-SCALE PLATFORMS . . . . .	11
A. The beginnings of the Brillouin scattering research field . . . . .	3	A. SBS in chalcogenide waveguides . . . . .	11
B. Characteristics of freely propagating BLS . . . . .	5	B. SBS in silicon . . . . .	12
C. Brillouin imaging for 3D micromechanical mapping of tissues, cells, and biomaterials . . . . .	5	C. SBS in high-Q resonators . . . . .	14
IV. STIMULATED BRILLOUIN SCATTERING IN OPTICAL FIBER . . . . .	5	D. Emerging material platforms . . . . .	14
A. SBS in telecommunications . . . . .	8	E. Brillouin interactions driven via transducers . . . . .	15
		VI. APPLICATIONS OF ON-CHIP SBS . . . . .	16
		A. SBS for integrated microwave photonic signal processing . . . . .	16

B. SBS for integrated optical signal processing and generation . . . . .	18
VII. FUTURE PERSPECTIVE—CHALLENGES AND OPPORTUNITIES . . . . .	19

## I. INTRODUCTION AND OUTLINE

The Year 2022 is the 100th anniversary since Leon Brillouin theoretically described the interaction between light and sound waves.<sup>1</sup> The effect, now known as Brillouin scattering, is one of the strongest nonlinear optical effects and was observed in multiple different platforms, from kilometer-long optical fibers,<sup>2</sup> chip-integrated microstructures<sup>3</sup> to biological tissue.<sup>4</sup>

The large variety of platforms explored and developed over the century of research into Brillouin scattering is a testimony of the many applications it underpins. Distributed temperature and strain sensors based on Brillouin scattering are now installed in critical infrastructure, from bridges to pipelines, tunnels, and skyscrapers.<sup>5–7</sup> Its impact on optical signal processing and microwave photonics (MWP) in optical fiber has been demonstrated in many groundbreaking research demonstrations, and any telecommunication system needs to consider and mitigate the effects of Brillouin scattering.<sup>2</sup>

Recent trends see Brillouin scattering harnessed on chip-scale platforms. Microscale waveguides engineered to guide acoustic and optical waves enable new ways to control and manipulate optical signals in a small footprint.<sup>3</sup> On the other hand, micrometer resolution Brillouin microscopes offer unique insight into the stiffness of cells and biological tissue.<sup>4</sup>

This review gives an overview of 100 years of Brillouin research, from the initial theoretical prediction to current trends and opportunities. We start with a historical development highlighting the seminal research papers that serve as the foundation of recent studies. As outlined in this introduction, the Brillouin research community is highly diverse and spans many platforms and applications. For the sake of structuring this review, we categorized the development of the field into three themes, which are all ongoing lines of research to the current day and are visualized in Fig. 1.

The first theme deals with Brillouin scattering in non-guiding media that includes initial demonstrations in gases and liquids that formed the basis for current research in Brillouin microscopy and biomedical characterization of biological tissues.<sup>4,34</sup>

The second theme covers Brillouin scattering in an optical fiber that provides long interaction lengths. The low-loss optical fiber platform is the backbone for many of the most mature applications in the field of Brillouin light scattering (BLS), such as distributed sensing and signal processing, and is still an active field of research. It has also been studied extensively in the context of optical communication systems, where Brillouin scattering was mainly seen as a nuisance for a long time.<sup>35</sup>

The most recent third theme can be labeled as Brillouin scattering in microstructured waveguides. The ability to alter waveguides on a microscopic level opened the door to tailor the interaction between optical and acoustic modes, which is interesting from a fundamental physics point of view but also enables promising applications in a small footprint.

As this review lays out the three themes, we cover the different platforms explored and developed along the way, as well as applications. We highlight the performance metrics achieved so far but also keep an eye on the future and the challenges ahead. At the end of the review, we give a consolidated outlook of where we see the field of Brillouin research heading. Given how far the field has come over the last 100 years and the large community of researchers working on Brillouin scattering today, we are filled with anticipation with the thought of what the next 100 years will bring.

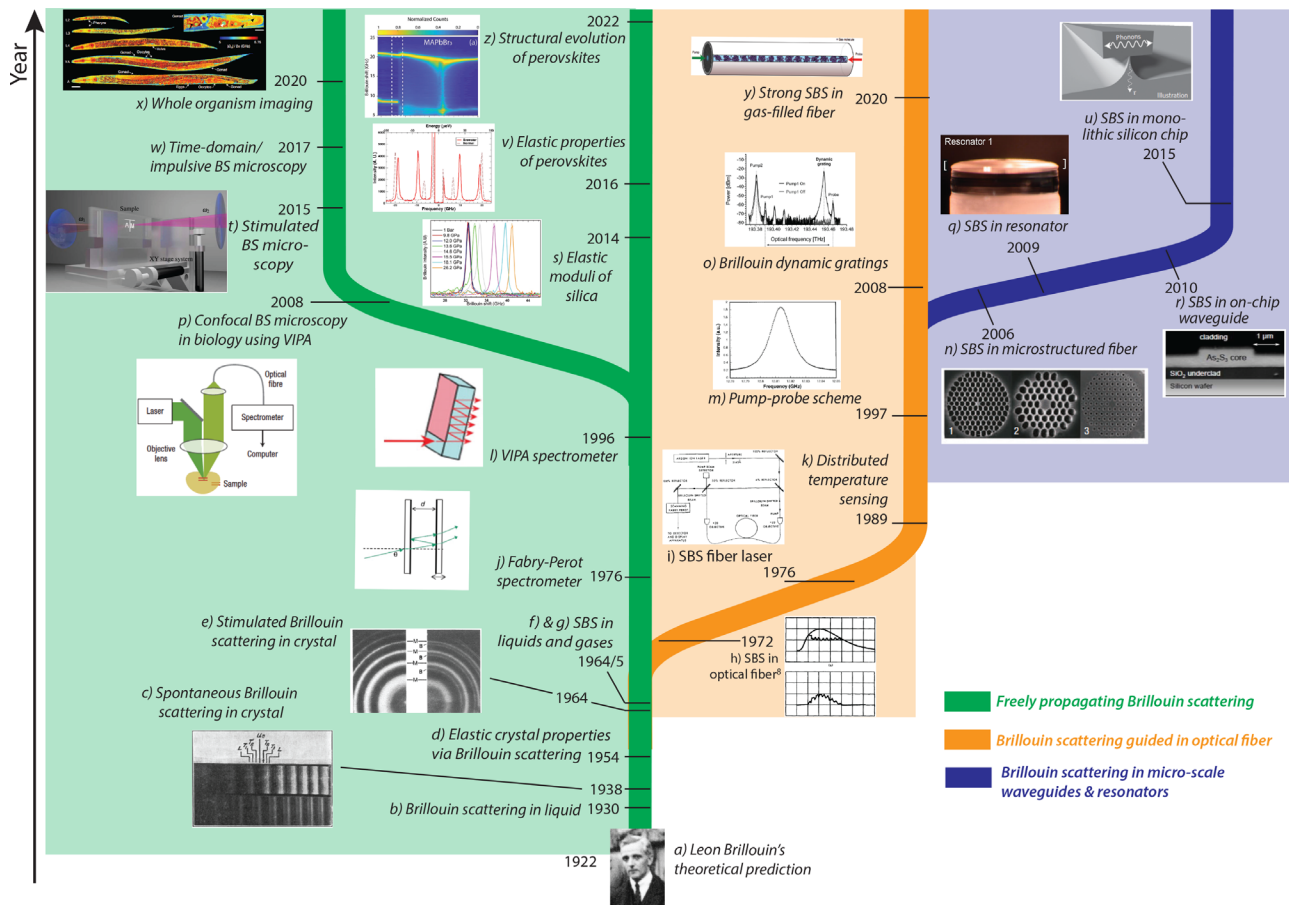
## II. HISTORICAL DEVELOPMENT OF DIFFERENT PLATFORMS

The phenomenon of Brillouin light scattering is named after Leon Brillouin<sup>1</sup> who described in 1922 the interaction of optical waves with acoustic waves in a medium. Independently of Brillouin, Mandelstam conducted similar studies in Russia and published his description of the scattering process in 1926.<sup>36</sup> Consequently, parts of the literature use the terminology “Brillouin-Mandelstam scattering.” For the rest of this review paper, however, we refer to the effect as “Brillouin scattering” or “stimulated Brillouin scattering (SBS)” depending on whether the scattering process occurs spontaneously or is stimulated, respectively.

In the most general sense, Brillouin scattering describes the scattering of an optical wave from an acoustic wave where the acoustic wave can be a longitudinal pressure/density wave in a solid, gas, or liquid, an acoustic surface wave, or a transverse acoustic wave Figs. 2(a) and 2(b).<sup>37</sup> When an optical wave is scattered from the acoustic wave, a frequency-shifted optical wave is generated, called the Stokes wave when lower in frequency than the pump wave and the anti-Stokes wave when at a higher frequency.<sup>37</sup> This process can be stimulated, which leads to an exponential gain of the optical Stokes wave, as shown in Figs. 2(c)–2(f). Here, a small optical seed that counterpropagates the optical pump creates an optical beat pattern. The small seed can be a laser coupled from the opposite side into the medium than the pump or originate from the scattering of the pump from thermal phonons. When the frequency separation of the pump and the seed matches the Brillouin frequency shift (BFS) in the medium, then the optical beat pattern reinforces the acoustic wave via electrostriction, which, in return, amplifies the seed/Stokes wave via scattering of the optical pump from the moving acoustic wave. This feedback can create strong amplification of the initially weak seed/Stokes wave. The corresponding spectral amplitude response is shown in Fig. 2(f). In addition to backward Brillouin scattering, an interaction between optical and acoustic waves can also be induced with co-propagating optical signals; however, the nature of the acoustic wave is then mainly transverse.

The field of Brillouin research has seen several phases and themes that can be roughly categorized in the following way:

- Theme 1 started in the 1920s with the first theoretical predictions and early experimental investigations of *spontaneous* scattering processes and later *stimulated* Brillouin scattering processes in liquids, gases, soft matter, glasses, and crystalline solids.
- Theme 2 started in the 1970s with the study of SBS in the recently developed low-loss optical fiber that enabled long interaction lengths. The research focus lays on developing SBS



**FIG. 1.** Development of Brillouin scattering research from its initial prediction until today following seminal research results along the three different themes outlined in the introduction, Brillouin scattering freely propagating, in long length of optical fiber, and in micro-scale waveguides. (a) Leon Brillouin at Solvay conference 1927; (b) reported in Ref. 8; (c) Reprinted with permission from C. V. Raman and C. S. Venkateswaran, *Nature* **142**, 250–250 (1938). Copyright 1938 Springer Nature;<sup>8</sup> (d) reported in Ref. 10; (e) Reprinted with permission from Chiao *et al.* *Phys. Rev. Lett.* **12**, 592–595 (1964). Copyright 1964 American Physical Society;<sup>11</sup> (f) reported in Refs. 12 and 13; (g) reported in Ref. 14; (h) Reprinted with permission from E. Ippen and R. Stolen, *Appl. Phys. Lett.* **21**, 539 (1972). Copyright 1972 AIP Publishing LLC;<sup>15</sup> (i) Reprinted with permission from Hill *et al.*, *Appl. Phys. Lett.* **28**, 608 (1976). Copyright 1976 AIP Publishing LLC;<sup>16</sup> (j) reported in Ref. 17; (k) reported in Ref. 18; (l) reported in Ref. 19; (m) Reprinted with permission from Nikles *et al.* *IEEE J. Lightwave Technol.* **15**, 1842–1851 (1997). Copyright 1997 IEEE;<sup>20</sup> (n) Reprinted with permission from Dainese *et al.*, *Nat. Phys.* **2**, 388–392 (2006). Copyright 2006 Springer Nature;<sup>21</sup> (o) Reprinted with permission from Song *et al.*, *Opt. Lett.* **33**, 926 (2008). Copyright 2008 The Optical Society;<sup>22</sup> (p) Reprinted with permission from G. Scarcelli and S. H. Yun, *Nat. Photonics* **2**, 39–43 (2008). Copyright 2008 Springer Nature;<sup>4</sup> (q) Reprinted with permission from Grudinin *et al.*, *Phys. Rev. Lett.* **102**, 043902 (2009). Copyright 2009 American Physical Society;<sup>23</sup> (r) Reprinted with permission from Pant *et al.* *Opt. Express* **19**, 8285–8290 (2011). Copyright The Optical Society;<sup>24</sup> (s) Adopted from Ref. 25; (t) Adopted from Ref. 26; (u) Reprinted with permission from Van Laer *et al.*, *Nat. Photonics* **9**, 199–203 (2015). Copyright 2015 Springer Nature;<sup>27</sup> (v) Adopted from Ref. 28; (w) Reported in Refs. 29 and 30, respectively; (x) Reprinted with permission from Remer *et al.*, *Nat. Methods* **17**, 913–916 (2020). Copyright 2020 Springer Nature;<sup>31</sup> (y) Reprinted with permission from Yang *et al.*, *Nat. Photonics* **14**, 700–708 (2020). Copyright 2020 Springer Nature;<sup>32</sup> (z) Adopted from Ref. 33.

applications as well as mediating and reducing detrimental SBS effects in optical data transmission systems.

- Theme 3 started around 2000 with major research efforts focused on controlling and harnessing SBS in micro-structured waveguides and integrated chip-scale platforms.

The remainder of this review paper will be structured following these three broad categories: Brillouin scattering without guidance, Brillouin scattering in optical fibers, and Brillouin scattering in micro-structured waveguides. Despite being developed and studied successively over time, all have found significant

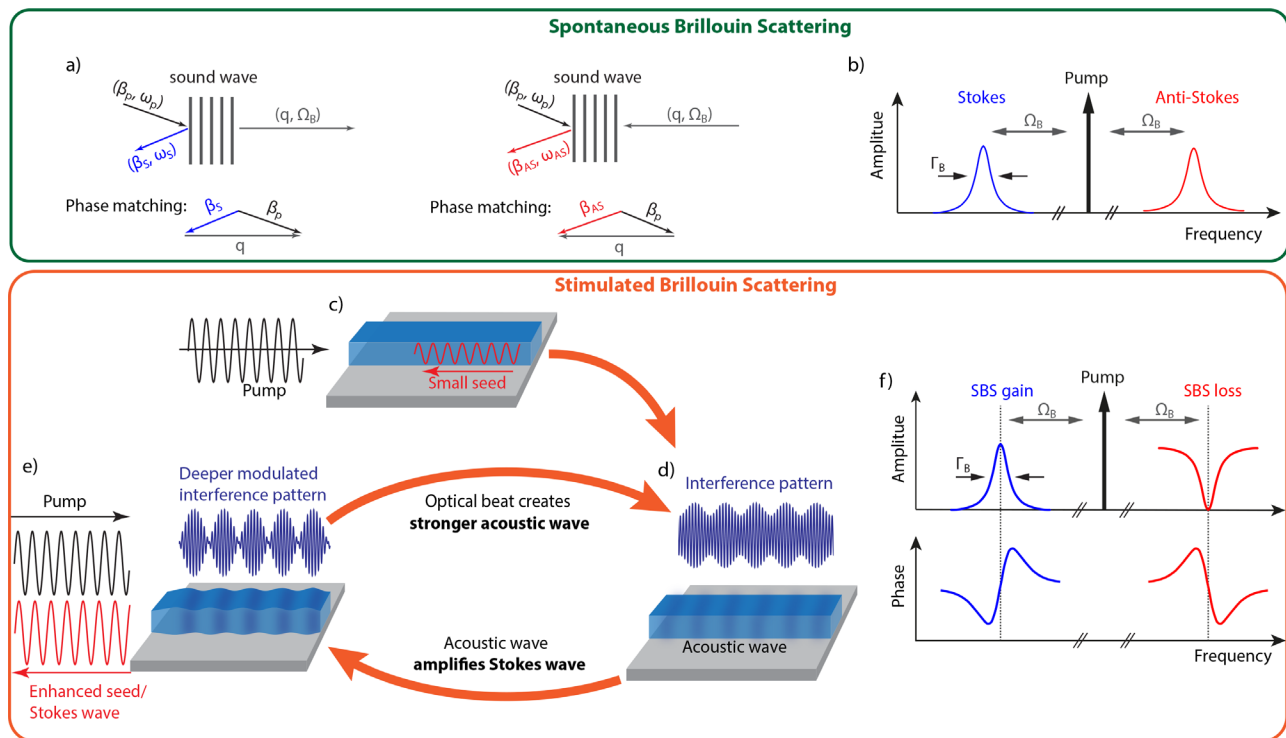
applications today, such as Brillouin microscopy, remote sensing, and chip-based signal processing.

### III. BRILLOUIN SCATTERING IN GASES, CRYSTALS, LIQUIDS, AND BIOLOGICAL MATERIALS

#### A. The beginnings of the Brillouin scattering research field

The initial period of Brillouin research, due to a lack of coherent light sources, focused on *spontaneous* inelastic scattering of light from acoustic vibrations. First, experimental observations of inelastic light





**FIG. 2.** (a) Spontaneous Brillouin scattering and phase matching for the Stokes and anti-Stokes wave. (b) Optical pump and spectral response of the Stokes and anti-Stokes wave. (c)–(e) Stimulated Brillouin scattering. (c) An optical pump interacts in the medium with a counterpropagating seed at the Brillouin frequency shift. (d) When the optical beat generated by said tones matches the Brillouin frequency shift, electrostriction induces an acoustic wave, (e) which creates a stronger Stokes wave. The now deeper optical modulation generates a stronger grating. (f) Stimulated Brillouin scattering gain and loss.

scattering from molecular vibrations were reported by Raman in the 1920s<sup>38–40</sup> and demonstrations of Brillouin scattering from acoustic density waves followed shortly.<sup>8,9,41,42</sup>

Today, one distinguishes between Raman and Brillouin scattering depending on the dynamics of the scattering process, or in other words, the type of “phonon,” a term introduced by Tamm in the 1930s<sup>43</sup> to describe fundamental quanta of lattice vibrations, that is involved in the scattering process.

The pressure waves, which function as scatterers in the case of backward Brillouin scattering, are termed *acoustic* phonons and show a linear dispersion relation in bulk, but can be altered in waveguides. The molecular vibrations studied in Raman scattering have a flat dispersion and are known as *optical* phonons. Based on the similarity of the phonon dispersion, forward Brillouin scattering (FBS) is sometimes referred to as Raman-like scattering.<sup>44</sup>

The magnitude of the frequency shift of the scattered Stokes wave depends on the properties of the acoustic wave and hence the elastic properties of the material. Not surprisingly, one of the first applications of Brillouin light scattering (BLS) was the characterization of crystal structures and structural defects<sup>10</sup> to complement x-ray diffraction measurements. Spontaneous BLS is still being used extensively in the characterization of novel glassy and crystalline materials; for example, perovskite crystals developed specifically for solar energy applications.<sup>28,45</sup>

A new paradigm in the field of Brillouin scattering, as in many other fields, started with the development of the laser at the beginning

of the 1960s.<sup>46</sup> The pristine coherence properties and the high power levels of the laser enabled researchers, for the first time, to reach the regime of *stimulated* Brillouin scattering (SBS).<sup>47</sup>

The first demonstration of SBS was reported in 1964 in Quartz and Sapphire crystals,<sup>11</sup> followed by demonstrations of SBS in liquids<sup>12,13,48</sup> and in gases.<sup>14</sup> Shortly after, a theoretical description of the effect was reported by Kroll based on a classical model of electrostriction and photoelasticity.<sup>49</sup> Tang further expanded Kroll’s theory taking into account the nonlinear relationship between the coupled waves, such as saturation.<sup>50</sup> Furthermore, Tang derived an expression for the strength of the coherent acoustic wave<sup>50</sup> and the first experimental and theoretical investigation of the phonon lifetime was reported a few years after.<sup>51</sup>

Figure 1 summarizes conceptual and technological developments in BLS technology and applications and maps milestone demonstrations within this fascinating field of research. Broadly, we separate the evolution of BLS technology and applications into three themed branches: (1) Brillouin scattering interactions between freely propagating light and hypersound, (2) BLS guided in optical fibers, and (3) BLS in integrated photonic circuits and micro-resonators. Each category will be discussed in detail in the rest of this review. In Sec. III B, we start by focusing on the physical principles behind freely propagating BLS and its applications in solids, liquids, and soft matter. Soft matter is an umbrella term that describes both man-made soft materials such as

polymers (e.g., hydrogels) as well as biological matter such as tissues and cells.

## B. Characteristics of freely propagating BLS

Irrespective of the material, the key outputs of any BLS experiment are the Brillouin frequency shift ( $\Omega$ ) and the Brillouin linewidth ( $\Gamma$ ). The Brillouin frequency shift (BFS) is directly proportional to the velocity of hypersound waves  $V$  as  $\Omega = \pm Vq$ , where  $q = \frac{4\pi n}{\lambda} \sin \Theta/2$  is the phonon wave number,  $n$  is the material refractive index, and  $\Theta$  is the scattering angle. Traditionally, Brillouin scattering experiments are set up in a back-scattering geometry; thus,  $V$  is related to the material's p-wave modulus  $M$  (also known as the longitudinal elastic modulus) and the material density  $\rho$  as  $V = \sqrt{M/\rho}$ . The changes in BFS can therefore indicate changes in material elasticity, density, or local refractive index.<sup>4</sup> Compared to solids, biological tissues and cells are mostly soft and full of water (over 70% of tissues' content on average). High levels of hydration are attributed to the low BFS in soft matter compared to solids such as glasses and crystals.<sup>52</sup> For example, the cell cytoplasm has a BFS of 7.6 GHz (when probed with  $\lambda = 532$  nm laser light),<sup>53</sup> and dehydrated fibrous components of muscles and tendons have a BFS in the range of 10–20 GHz,<sup>54</sup> which is still significantly lower than the typical BFS in glasses, that is, 25–30 GHz for the same laser wavelength.

In addition, the Brillouin linewidth  $\Gamma = 1/\tau$  is inversely proportional to the phonon lifetime and provides an indication of several material properties, including material heterogeneity and phonon loss.<sup>55</sup> Both parameters are of key importance for material science and help to improve the purity of the material composition as well as optimize energy dissipation of light on interactions with atomic lattice vibrations.<sup>56</sup> In soft matter, however, high hydration levels and interactions between solid and liquid phases of a poro-elastic compound material lead to another important source of energy dissipation that can broaden the Stokes and anti-Stokes Brillouin lines, namely, viscous damping. Therefore, in liquids and soft matter,  $\Gamma$  often serves as a measure of local dynamic viscosity  $\eta$ , that is,  $\Gamma \propto \eta$ . Typical widths of Brillouin peaks in tissues, biological liquids, and gels are from 500 MHz to a few GHz,<sup>53,55</sup> depending on the material composition and structure, which is at least an order of magnitude larger than Brillouin linewidths found in solid-state crystalline materials (10–100 MHz).<sup>51</sup>

## C. Brillouin imaging for 3D micromechanical mapping of tissues, cells, and biomaterials

The beginning of the 21st century has seen an explosion of interest in imaging technology with the goal to resolve nanoscopic details of living matter<sup>69,70</sup> and the structure of macromolecules,<sup>71</sup> as well as to characterize optical, chemical and mechanical properties of matter at once by combining several imaging modalities together.

At the same time, Brillouin light scattering spectroscopy has also evolved into 3D imaging, known as Brillouin microscopy, through the optimization of Brillouin spectrometers,<sup>4,72</sup> and their combination with confocal microscopy systems.<sup>4</sup> The transition from point measurement spectroscopy to scanning microscopy required an improvement of the measurement speed, which was achieved by transitioning from fairly slow scanning Fabry–Pérot interferometers<sup>73</sup> to motor-free angular etalons such as virtually imaged phase arrays (VIPAs) for

detecting the Brillouin signals.<sup>72</sup> Such a transition allowed to speed up the signal acquisition process from tens of seconds to tens of milliseconds, enabling fast mapping of tissues and cells, albeit with a loss of spectral resolution and signal quality.<sup>74,75</sup>

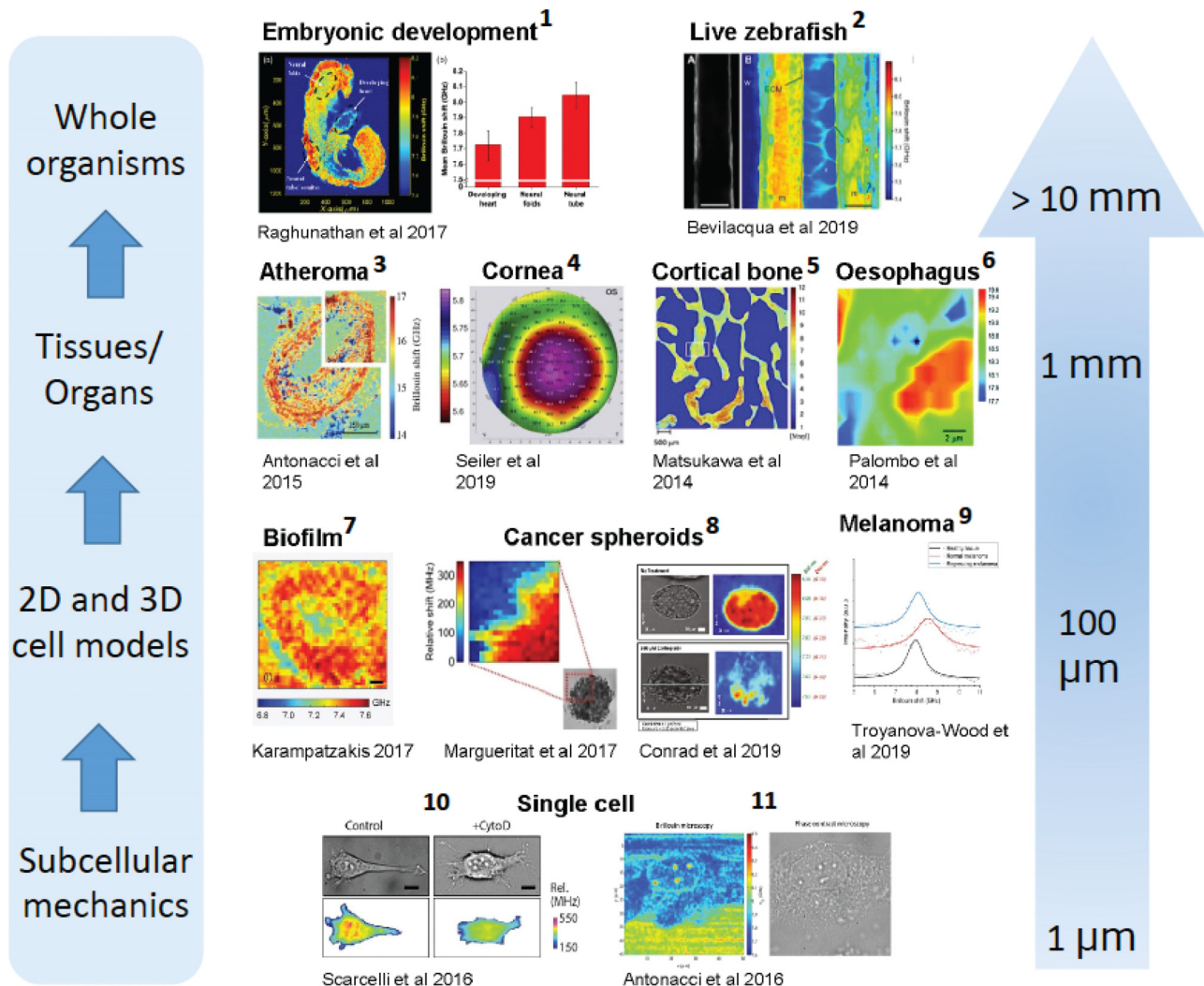
3D Brillouin imaging has significantly evolved in the past 20 years, adopting technologies from telecommunications such as SBS<sup>76</sup> to improve scattering efficiency and from fast optical microscopy such as line-scanning Brillouin microscopy.<sup>67</sup> Improvements in imaging speed and signal-to-noise ratio (SNR) enabled *in vivo* measurements of whole macroscopic organisms, for example, *C. elegans*, with the spatial resolution down to cellular level and shot-noise limited detection.<sup>31</sup> To date, Brillouin micro-spectroscopy and microscopy have been applied to the full range of biological samples from proteins and fibrous matrix components,<sup>54</sup> to single cells,<sup>53</sup> organs and whole organisms<sup>31</sup> as illustrated in Fig. 3.

Despite the striking progress in this field, a number of challenges remain open and require further research and development. Briefly, the Brillouin image acquisition speed is still incompatible with live cell imaging, thus asking for continuing invention and optimization. It is worth noting that the current record acquisition speed of 2 ms per point is already limited by shot-noise and can no longer be improved in classical measurement schemes. This limitation demands novel approaches based on quantum detection using non-classical states of light<sup>77</sup> or breakthroughs in signal processing techniques, for example, the ones based on compressive imaging where the number of measurement points per sample can be reduced without loss of image quality through image reconstruction algorithms.<sup>78</sup>

Another limitation of Brillouin imaging that needs special notice is related to the spatial resolution of this technology. Because Brillouin imaging is based on the interactions between photons and phonons, improvements of the setup to reach optical diffraction-limited imaging not always pay off as the spatial resolution is fundamentally limited by the properties of the hypersound wave, such as its attenuation length and wavelength. For the majority of biological matter, the attenuation length is above 1  $\mu\text{m}$ , exceeding both the sound wavelength and the optical diffraction limit by a few folds. This phonon attenuation length imposes a limit on the spatial resolution, as all phonons from the spherical volume within the radius equal to the attenuation length are detected in the measurement process.<sup>55</sup> Phonon spatial confinement and phonon resonances can be a way to improve phonon localization and achieve finer measurement resolution. Some of these ideas will be discussed further in relation to data transmission and processing in photonic integrated circuits in Sec. V.

## IV. STIMULATED BRILLOUIN SCATTERING IN OPTICAL FIBER

The first observation of SBS in optical fiber was reported in 1972,<sup>15</sup> which was made possible by the development of optical fibers that could guide light for several kilometers with losses now as low as 0.2 dB/km.<sup>82</sup> Interestingly in this demonstration, the author described SBS as a limiting factor for communication systems: “SBS limits the amount of narrow-band power which one can transmit through a fiber,” which indicates that from an early stage, SBS was considered as a nuisance in optical communication systems. The reason for this negative sentiment is that even moderate continuous wave (CW) pump powers could reach the SBS threshold and amplify the Stokes wave traveling in the backward direction.



**FIG. 3.** Evolution of biological structures that can be probed using Brillouin scattering. Adapted from (1) Ref. 57, (2) Ref. 58, (3) Ref. 59, (4) Ref. 60, (5) Ref. 61, (6) Ref. 62, (7) Ref. 63 (8) Refs. 64 and 65, (9) Ref. 66, (10) Ref. 67, and (11) Ref. 68.

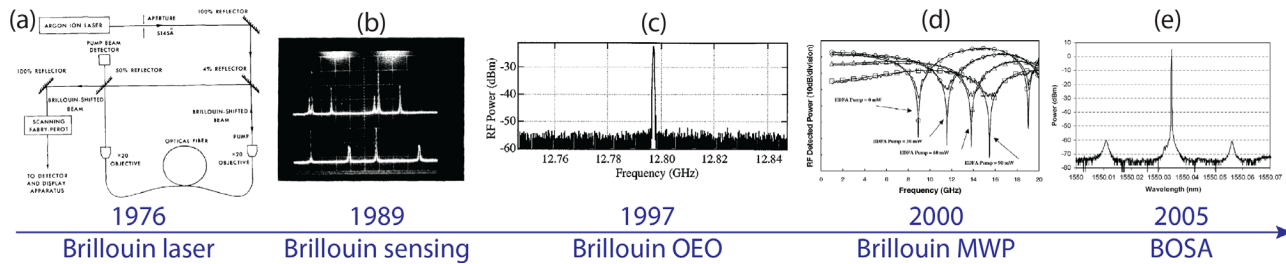
In a further study, Smith investigated the Brillouin threshold in optical fibers for the backward scattering process.<sup>83</sup> This critical power below which the stimulated Brillouin effect may be neglected (Brillouin threshold) depends upon the effective core area, propagation loss, and gain coefficient in optical fibers. Later, Boyd *et al.*<sup>84</sup> derived a theoretical model for what is known as the SBS generator configuration where SBS is initiated from thermally excited acoustic phonons and showed how the Stokes linewidth and intensity are dependent upon the physical properties of the SBS medium.

The low SBS threshold power was soon utilized to demonstrate the first Brillouin laser<sup>16</sup> using a fiber loop as a laser cavity [see Fig. 4(a)], followed by the demonstration of the first cascaded Brillouin laser.<sup>85</sup> In addition, a very low-threshold all-in-fiber Brillouin laser with a sub-milliwatt threshold was demonstrated in 1982 by Stokes *et al.*<sup>86</sup>

The Brillouin effect in fiber was further utilized to demonstrate the first semiconductor laser-pumped Brillouin fiber amplifier in 1987 by Olsson *et al.*<sup>87</sup> In this study, a broad-bandwidth Brillouin fiber amplification was demonstrated by applying a frequency modulation (FM) to the pump laser. Shortly after that, Lichtman *et al.* studied the effect of modulated pump on the SBS threshold and gain.<sup>88</sup> In 1992, Gaeta *et al.* showed theoretically and experimentally the threshold required to start a Brillouin oscillation in a cavity and demonstrated the Stokes linewidth narrowing above the threshold for Brillouin oscillation.<sup>89</sup>

From an early stage, SBS was used as a characterization tool for optical fibers. In 1989, Culverhouse *et al.* predicted that the Stokes frequency shift can be used as a means for distributed temperature sensing<sup>18</sup> [see Fig. 4(b)] and started a new chapter for Brillouin scattering applications as a sensing mechanism, which is discussed in more detail in Secs. IV B and IV C.





**FIG. 4.** Selection of different Brillouin applications in optical fiber since initial demonstration in 1972.<sup>15</sup> (a) Brillouin fiber laser,<sup>16</sup> (b) Brillouin distributed temperature sensing,<sup>18</sup> (c) Brillouin optoelectronic oscillator (OEO) as a narrowband microwave source,<sup>79</sup> (d) Brillouin MWP applications exemplified by Brillouin-based phase shifter,<sup>80</sup> and (e) high-resolution Brillouin optical spectrum analyzer (BOSA).<sup>81</sup> (a) Reprinted with permission from E. Ippen and R. Stolen, *Appl. Phys. Lett.* **21**, 539 (1972). AIP Publishing LLC.<sup>15</sup> (c) Reprinted with permission from X. S. Yao, *Opt. Lett.* **22**, 1329–1331 (1997). Copyright 1997 The Optical Society;<sup>79</sup> (d) Reprinted with permission from Loayssa *et al.*, *Opt. Lett.* **25**, 1234–1236 (2000). Copyright 2000 The Optical Society;<sup>80</sup> (e) Reprinted with permission from Domingo *et al.*, *IEEE Photonics Technol. Lett.* **17**, 855–857 (2005). Copyright 2005 IEEE.<sup>81</sup>

While Brillouin distributed sensing is one major driver of fiber-based Brillouin research and arguably the most mature technology in terms of commercial adaptation, the research community has started more and more to appreciate the unique properties of SBS for signal processing. This realization marks a shift from the initial perception of SBS as a nuisance in telecommunication systems toward offering a variety of functionalities for all-optical signal processing to enhance telecommunication systems as well as microwave photonics. The seminal demonstration of those processing functionalities in optical fibers, such as optical<sup>90,91</sup> and microwave photonic filtering,<sup>92–95</sup> all-optical delays,<sup>96–98</sup> and microwave photonic phase shifter,<sup>80,99</sup> set the foundation for many of the more recent on-chip demonstrations (outlined in Sec. V) that offers reduced size, weight, and power consumption, as well as cost (SWAP-C) through scalable manufacturing processes.

For both fiber and chip-based SBS applications, it is essential to characterize the Brillouin gain spectrum of the waveguide precisely. In 1997, Nikles *et al.* published a seminal paper on a pump–probe architecture based on a single laser and a modulator to sweep one of the optical sidebands across the Brillouin resonance.<sup>20</sup> Precisely, characterizing the narrow Brillouin gain spectrum via a pump–probe method is not only essential for calibrating optical fiber sensors but also to characterize the narrowband Brillouin response of different on-chip waveguide designs and material platforms and can nowadays be considered a “gold-standard” measurement.

The intrinsic narrow linewidth of SBS was identified as a powerful tool for microwave photonics (MWP), the research field that aims to process microwave signals by first transducing and then processing the microwaves in the optical domain.<sup>100</sup> Performing the signal processing in the optical domain offers great advantages in terms of bandwidth compared to the electronic domain; however, it often requires very fine-resolution optical signal processing techniques to act on the optical carrier or sidebands to manipulate the signals, which is challenging. The narrowband amplitude and phase response of the SBS gain and loss resonance, and the fact that it is tunable via the optical pump, make SBS a prime candidate for performing signal processing in the optical domain. Different MWP filter functionalities from, bandpass to bandstop and narrowband notch filters,<sup>92–95</sup> as well as broadband MWP phase shifters<sup>80,99</sup> have been demonstrated in optical fiber [a phase shifter is shown in Fig. 4(d) as an example for Brillouin MWP applications in optical fiber].

It was recognized that SBS could not only be used to manipulate microwave signals but also to efficiently generate stable microwave signals. In essence, all-optical approaches to generating microwave signals rely on beating two optical tones on a photodetector to generate the desired microwave tone. Brillouin scattering has been used in different configurations that, broadly speaking, can be summarized in two different categories: an optical pump generates a second (or more) optical tones via SBS that beat on a photodetector, as, for example, in a Brillouin fiber laser approach.<sup>101–103</sup> The alternative approach relies on SBS as a filter that selects the optical tones that beat on the photodetector; this could either be in conjunction with an optical frequency comb<sup>104</sup> or as an active filter in an optoelectronic oscillator (OEO).<sup>79</sup> A stable microwave tone generated by the Brillouin OEO is shown in Fig. 4(c).

In 2005, it was realized that Brillouin scattering in optical fiber could be used to delay optical signals.<sup>96,97</sup> As often in the history of scientific discovery, the effect was reported almost simultaneously by two independent research groups. The realization that optical signals can be slowed down, an effect commonly referred to as “slow-light,” at room temperature utilizing off-the-shelf telecommunications components presents an important step toward the realization of an optical buffer that could avoid the electronic to optical conversion. However, it was soon realized that SBS slow-light has a limited time-bandwidth product and can only delay a small number of optical bits<sup>105</sup> and is limited by pulse distortions.<sup>106,107</sup>

In the following years, researchers pursued different approaches to overcome the limitations of slow-light. In 2007, Zhu *et al.* reported light storage based on SBS.<sup>98</sup> In this approach, the optical data pulses are not slowed down by the dispersive phase slope of the SBS resonance but are rather transferred to the acoustic wave via the resonant interaction between the optical data pulse and a second optical pump offset by the Brillouin frequency shift. Quasi-light storage (QLS) offers an alternative approach, where the optical data signal gets sampled by a frequency comb where SBS plays the role of achieving an optical convolution of the two signals, which leads to a train of copies of the signal in the time domain.<sup>108–110</sup> A different approach to delay signals using SBS harnesses the dynamic grating created in the SBS process as an optically induced Bragg reflector in an optical fiber.<sup>111–113</sup> The amount of delay is given by the position in the fiber at which the optical pump pulses that induce the grating meet.



A sometimes overlooked property of SBS is its sensitivity and interplay with the polarization of the two optical waves involved in the SBS process. In fact, the effects of the polarization of the optical waves in the Brillouin process have been known since the early experiments in optical fiber when Stolen reported in 1979 an increase in the Brillouin gain of a factor of 2 when linear polarization of the optical waves is maintained along the fiber.<sup>114</sup> Over the following decades, the effect of polarization on SBS was investigated in different fiber types, from standard single mode,<sup>115,116</sup> to different types of birefringent fibers,<sup>117</sup> and Brillouin laser configuration.<sup>118</sup> In 2008, Zadok *et al.* presented a vector analysis of SBS in the presence of birefringence.<sup>119</sup> More recently, it was shown that SBS can be used for all-optical polarization control in a wavelength-selective manner.<sup>120</sup>

The polarization effects of SBS were harnessed to enhance optical filters<sup>121</sup> that were also used in optical spectrum analyzers based on SBS.<sup>122,123</sup> Brillouin optical spectrum analysis, known as BOSA, offers unprecedented resolution compared to traditional grating-based spectrum analyzer<sup>81</sup> and was successfully commercialized.<sup>124</sup> A high-resolution spectrum measured via BOSA is shown in Fig. 4(e). The performance of the Brillouin-based spectrum analyzer has been increased to reach the sub-MHz regime by utilizing Brillouin dynamic gratings.<sup>125</sup> More recently, it was shown that the polarization effects of SBS combined with interference can lead to very narrow spectral dips within the Brillouin gain resonance in twisted birefringent fiber,<sup>126</sup> as well as standard single-mode fiber.<sup>127</sup>

### A. SBS in telecommunications

The early realization of SBS being a potential hindrance turned out to be a significant challenge in communication systems, with major research efforts undertaken to mediate or suppress SBS.<sup>128–138</sup> Different approaches were pursued by scientists and range from the development of specialty fiber<sup>133</sup> to applying heat and stress gradients<sup>134,139</sup> along fiber spools. Other techniques are based on purposely jittering the optical pump<sup>140</sup> or periodically interrupting the fibers with isolators<sup>141</sup> to avoid the build-up of the Stokes wave.

Recently, however, researchers have started investigating the potential benefits of harnessing SBS in communication systems. In particular, in densely packed wavelength multiplexed systems, the ability to provide narrowband amplification offers great benefits.<sup>142,143</sup> Multiple fiber- and chip-based demonstrations have shown improvements in system performance using SBS for optical carrier recovery. In optical carrier recovery, SBS is utilized as an active and narrowband filter at the receiver side of a communication system to trace actively and filter the optical carrier, which then can be used as a local oscillator to demodulate the signal.<sup>144–147</sup>

In addition to the narrow bandwidth of the SBS gain to select optical carriers, the optical tunability across the whole telecommunication band in a continuous way makes it particularly useful for emerging wavelength multiplexed systems that are utilizing optical frequency combs. In those wideband systems, however, the dispersion of the Brillouin frequency shift is starting to play a significant role, which causes a detuning from the center of the Brillouin resonance for separate frequency comb lines. A solution to this problem was shown recently by Ref. 148 who demonstrated that broadening the SBS filter response overcomes the issue of frequency detuning due to the dispersion of the Brillouin frequency shift.

### B. Distributed sensing using backward Brillouin scattering

Brillouin scattering has long been used for distributed sensing, and given the growth of this area of SBS research, the level of maturity the technology reached, and its commercial importance, we provide a dedicated section to distributed Brillouin-based sensing that gives an overview of different techniques developed over the years. Since Brillouin is an inelastic scattering process, environmental changes such as temperature and strain directly affect the Stokes wave's properties. Therefore, frequency shift, intensity, and linewidth of the Stokes and anti-Stokes waves can be used for sensing strain, temperature, and the surrounding medium along an optical fiber.

Temperature-dependent Brillouin scattering was studied as early as 1989,<sup>162</sup> and in 1990, Brillouin distributed measurements of temperature and strain were reported by Kurashima *et al.*<sup>149</sup> and Horiguchi *et al.*<sup>163</sup> Bao *et al.*<sup>150</sup> and Nikles *et al.*<sup>164</sup> were also among the first to report distributed Brillouin sensing in optical fibers.

A common technique for distributed Brillouin sensing is based on time of flight, in which optical pulses are launched into the fiber and variations in the Brillouin frequency shift caused by environmental changes are measured as a function of time.<sup>165</sup> Both stimulated and spontaneous Brillouin scattering can be utilized in this way for distributed sensing along the fiber. The approach based on spontaneous Brillouin scattering is favorable in certain situations since it only requires access to one end of the fiber and is known as Brillouin optical time domain reflectometry (BOTDR).<sup>166,167</sup> The spatial resolution using this technique, however, is limited to around 1 m, which is dictated by the phonon lifetime in optical fibers (10 ns).<sup>6,151</sup>

Time-domain distributed sensing based on the *stimulated* Brillouin process is called Brillouin optical time domain analysis (BOTDA).<sup>149,150,164</sup> BOTDA has, in principle, the same limitation in terms of minimum optical pulse width as BOTDR imposed by the phonon lifetime,<sup>151</sup> however, different modified time domain techniques have been developed over the years to improve spatial resolution and measurement range significantly. A modification of BOTDA allows for higher spatial resolution (<1 m), called Brillouin echo-distributed sensing (BEDS),<sup>154,168,169</sup> by pre-exciting acoustic waves in the medium via a long pump pulse and therefore overcoming the limitation set by the phonon lifetime/build-up time. A sudden change in amplitude or phase of a delayed CW pump creates a highly localized Brillouin scattering response.<sup>6,153</sup> Several demonstrations based on this pre-excitation technique successfully achieved spatial resolution beyond the limitation of the phonon lifetime.<sup>152,170–172</sup>

Key performance criteria for distributed sensing systems include spatial resolution, measurement range, and the number of resolved points, as well as measurement time, frequency measurement accuracy, and signal-to-noise ratio (SNR). A trade-off exists between those performance metrics since improving one attribute often comes at the expense of deteriorating another; for example, a higher spatial resolution often means a weaker signal, shorter measurement range, and lower SNR. An expression for measurement accuracy and figure-of-merit based on performance criteria for BOTDA-based sensors is discussed in Ref. 173, while Ref. 7 looks into additional factors such as effects of random birefringence on measurement uncertainty.

Table I lists some of the techniques and advancements of time-domain distributed sensing, focusing on measurement range and spatial resolution. We note that this list intends to provide the reader of

TABLE I. Evolution of time-domain sensing techniques.

Reference	Technique	Spatial Res.	Measurement range	No. of resolved points <sup>a</sup>
163	BOTDA	100m	2 km	20
149	BOTDA	100m	1.2 km	12
166	BOTDR	100m	11.57 km	115
176	Raman-assisted BOTDR	15m	50 km	3333
177	Simplex-coded BOTDA	1 m	50 km	50 000
178	Dual-tone probe BOTDA	2 m	100 km	50 000
179	Time-division multiplexing-based BOTDA	2 m	100 km	50 000
180	Frequency-division multiplexing BOTDA	2 m	150 km	75 000
181	Double-pulse BOTDR	20 cm	1 km	5000
171	Brillouin dynamic grating	1 cm	20 m	2000
152	Dark-pulse BOTDA	5 cm	100 m	2000
154	BEDS	5 cm	5 km	100 000
182	Differential BOTDA	15 cm	1 km	6666
183	Differential BOTDA	1 cm	10 km	1 000 000
184	Pulse coding BOTDA	40 m	21 km	525
185	Simplex-coded BOTDA	3 m	120 km	40 000
186	Phase and amplitude coding BOTDA	2 cm	2.2 km	110
187	Genetic optimized BOTDA	2 m	39 km	19 500
188	Slope-assisted BOTDA	1.5 m	85 m	56
189	Slope-assisted BOTDA	2.5 m	2 km	800

<sup>a</sup>When not mentioned directly in the reference, “No. of resolved points” is evaluated as measurement range/spatial resolution.

this review on Brillouin scattering with an initial overview and cannot fully represent the massive amount of work that has been carried out in this domain over the years; for that, the reader is referred to the specialized literature, for example, Refs. 7, 174, and 175. The historical evolution of BOTDA-based sensors, performance advancements, and figure of merits are presented, for example, in detail in Ref. 173.

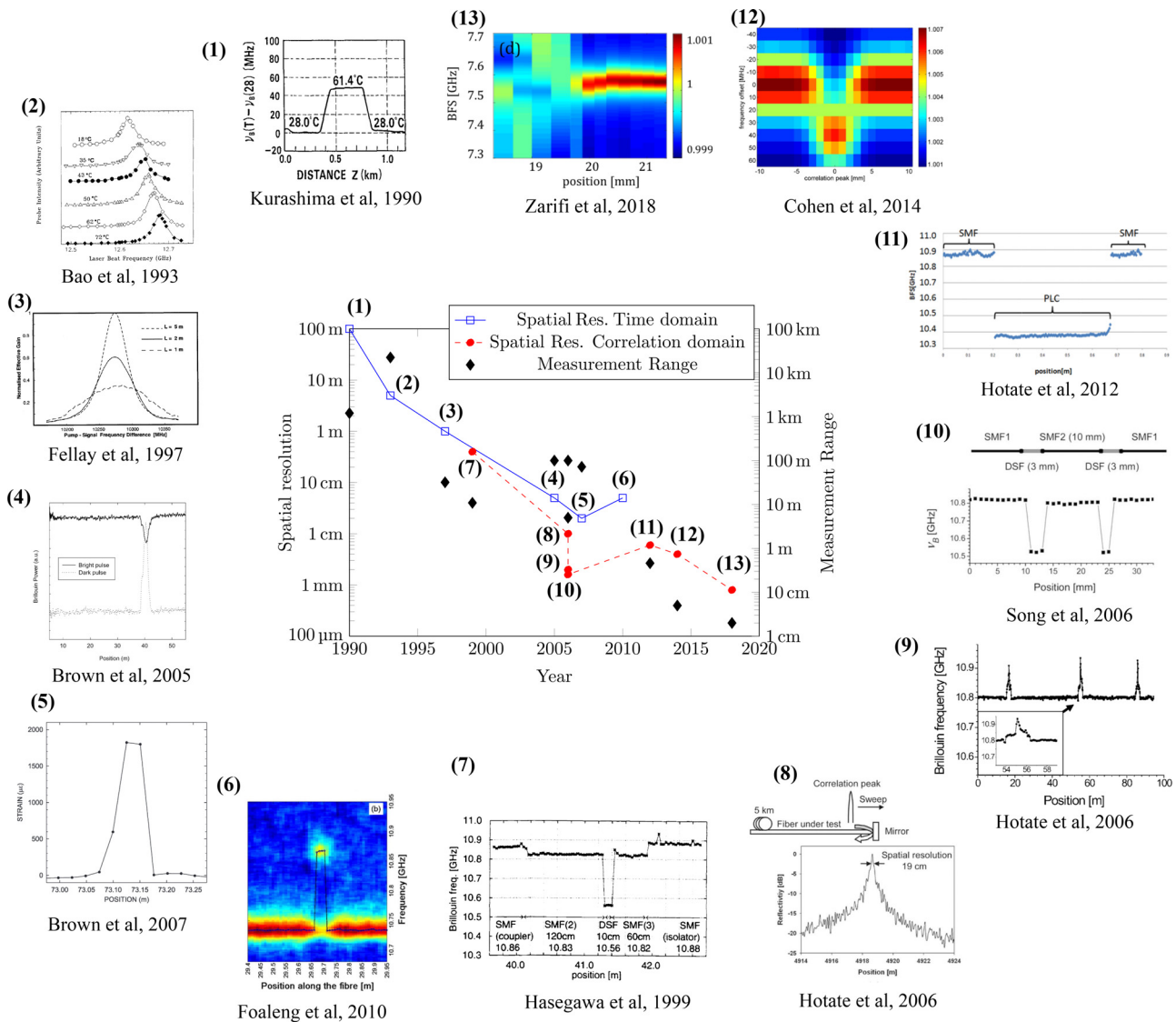
In addition to the above-described time domain sensing schemes, techniques based on Fourier analysis were proposed and demonstrated and are now known as Brillouin optical frequency domain analysis (BOFDA).<sup>190</sup> Here, a Brillouin response over time is obtained by applying a variable intensity modulation to the optical source.<sup>191</sup>

Brillouin optical correlation domain analysis (BOCDA) is another variation of distributed Brillouin sensing based on a low-coherence optical source. In this technique, the spatial resolution of the Brillouin response ( $\Delta z$ ) is defined by the coherence time ( $\Delta t$ ) of the source:  $\Delta z = \Delta t \cdot c/n_{\text{eff}}$ , where  $c$  is the speed of light and  $n_{\text{eff}}$  is the effective refractive index of the medium.<sup>192</sup> BOCDA was first demonstrated by Hotate and Hasegawa based on a frequency-modulated optical source.<sup>155,193</sup> For this technique, the measurement range is limited by the periodicity of the frequency modulation applied to the pump and probe. Random phase coding of the pump and probe first reported by Zadok *et al.*<sup>192</sup> increased the measurement range beyond this restriction with a reported spatial resolution of 1 cm over 40 m of optical fiber. Later, this technique was used to map the non-uniformity of microwires.<sup>194</sup> Further improvements in terms of noise reduction were achieved by synthesizing the auto-correlation function

to suppress off-peak Brillouin interactions from contributing to the BOCDA response.<sup>195</sup> A combined time-domain and correlation-domain approach has improved sensing range while reducing the effect of off-peak Brillouin interaction.<sup>196,197</sup> Using a time and correlation domain hybrid approach achieved a measurement range of 17 km with a spatial resolution of 8 mm.<sup>197</sup>

Another interesting distributed sensing approach relies on Brillouin dynamic gratings (BDG), refractive index gratings generated by SBS in one polarization to Bragg reflect an optical wave in the orthogonal polarization.<sup>22,198</sup> The temperature and strain dependency of the fiber birefringence makes BDGs a powerful distributed sensing mechanism.<sup>199,200</sup> Simultaneous measurement of temperature and strain in a polarization-maintaining fiber has been demonstrated using BDGs<sup>201</sup> and 1-cm spatial resolution over 20 m of optical fiber has been achieved using this technique.<sup>171</sup> Simultaneous measurement of temperature and strain using spontaneous Brillouin scattering has been shown in 1997 by Parker *et al.*<sup>202</sup>

Figure 5 shows an overall improvement in spatial resolution while also considering the achieved measurement range. This plot indicates the trade-off between those two parameters of a distributed sensing system; as we move toward higher spatial resolution, the measurement range becomes, in general, shorter. It should be noted that the plot only shows a selection of references and cannot represent the whole field of distributed Brillouin sensing. The selected references represent an overall trend in the research field toward improving one of the key metrics of a distributed sensing system—spatial resolution. It illustrates the general progress of the field toward resolving smaller spatial features, be it for Brillouin



**FIG. 5.** Evolution of spatial resolution and measurement range over time for selected distributed Brillouin sensing demonstrations based on time domain and correlation domain techniques. Y axis (right): spatial resolution, and (left): measurement range. Figure panels in anti-clockwise direction: (1) Reprinted with permission from Kurashima *et al.*, *Opt. Lett.* **15**, 1038–1040 (1990). Copyright 1990 The Optical Society.<sup>149</sup> (2) Reprinted with permission from Bao *et al.*, *Opt. Lett.* **18**, 1561 (1993). Copyright 1993 The Optical Society.<sup>150</sup> (3) From Fellay *et al.*, *12th International Conference on Optical Fiber Sensors*. Copyright 1997 The Optical Society. Reprinted with permission from Optical Society.<sup>151</sup> (4) Reprinted with permission from Brown *et al.*, *IEEE Photonics Technol. Lett.* **17**, 1501–1503 (2005). Copyright 2005 IEEE.<sup>152</sup> (5) Reprinted with permission from Brown *et al.*, *J. Lightwave Technol.* **25**, 381–386 (2007). Copyright 2007 IEEE.<sup>153</sup> (6) Reprinted with permission from Foaeng *et al.*, *J. Lightwave Technol.* **28**, 2993–3003 (2010). Copyright 2010 IEEE.<sup>154</sup> (7) Reprinted with permission from T. Hasegawa and K. Hotate, *Proc. SPIE* **3860**, 306–316 (1999). Copyright 1999 SPIE.<sup>155</sup> (8) Reprinted with permission from K. Hotate and Z. He, *J. Lightwave Technol.* **24**, 2541–2557 (2006). Copyright 2006 IEEE.<sup>156</sup> (9) Reprinted with permission from Hotate *et al.*, *IEEE Photonics Technol. Lett.* **18**, 2653–2655 (2006). Copyright 2006 IEEE.<sup>157</sup> (10) Reprinted with permission from Song *et al.*, *Opt. Express* **14**, 5860–5865 (2006). Copyright The Optical Society.<sup>158</sup> (11) Reprinted with permission from Hotate *et al.*, *IEICE Tech. Rep.* **112**, 95 (2013). Copyright 2013 IEICE.<sup>159</sup> (12) Reprinted with permission from Cohen *et al.*, *Opt. Express* **22**, 12070 (2014). Copyright The Optical Society.<sup>160</sup> (13) Reprinted with permission from Zarifi *et al.*, *APL Photonics* **3**, 036101 (2018). Copyright 2018 AIP Publishing LLC.<sup>161</sup>

microscopy (Sec. III C) as described earlier or the small on-chip structures described later in this paper (Sec. V). For a more in-depth discussion of Brillouin-based fiber sensors beyond this paper, the reader is referred to comprehensive literature reviews by, for example, Bao *et al.*,<sup>7</sup> Motil *et al.*,<sup>174</sup> and Dong.<sup>175</sup>

### C. Distributed sensing using forward Brillouin scattering

A new regime of Brillouin scattering in optical fiber was discovered by Shelby *et al.* in 1985.<sup>203</sup> This type of Brillouin scattering utilizes transverse acoustic waves propagating from the center of the fiber

toward the cladding and scatter optical waves traveling inside the fiber core. The frequency shift resulting from this interaction is on the order of MHz and can be detected in the forward direction (optical pump and probe wave are co-propagating). This class of Brillouin scattering is called guided acoustic wave Brillouin scattering (GAWBS) or forward Brillouin scattering (FBS).

The unique properties of FBS allow sensing the surrounding of standard optical fiber. In this sensing technique, the transverse acoustic modes resonating between the core and the cladding boundaries are affected by the properties of the media surrounding the cladding, affecting the acoustic resonances' linewidth.<sup>204,205</sup> Only relying on standard optical fiber has certain advantages over substance detection schemes based on backward Brillouin scattering, which usually rely on specialty fibers like microfibers<sup>206</sup> and photonic crystal fibers.<sup>207–209</sup>

Several techniques have been proposed and experimentally demonstrated that the use of FBS as a distributed sensing technique based on the combined effect of OTDR<sup>204</sup> and BOTDA<sup>205</sup> with reported spatial resolution of 100 m over 3 km and 15 m over a 730 m of optical fiber, respectively. Other techniques with improved spatial resolution include broadband BOTDR-based<sup>210</sup> and BOTDA-based<sup>211</sup> techniques, with spatial resolution of 8 and 6 m, respectively. A more recent technique utilizes time-varying phase modulation (serrodyne modulation) and achieved a spatial resolution of 2 m over 500-m-long fiber with 250 resolved points.<sup>212</sup> Recently, a direct measurement technique for FBS was proposed and experimentally demonstrated sensing of substances outside of standard polarization-maintaining fiber with a spatial resolution of 60 m and 1.1 km range.<sup>213,214</sup>

## V. MICROMETER-SCALE WAVEGUIDES AND CHIP-SCALE PLATFORMS

A new paradigm in SBS research started in the early 2000s with the observation of SBS in microstructured fibers and on-chip waveguides.<sup>3</sup> For the first time, researchers could directly study and tailor the effect of waveguide geometry on the SBS gain, which is determined by the overlap integral between the guided optical and acoustic waves. This theme of SBS research is exciting as, on the one hand, it can lead to new scientific insight into the interplay of optical modes with traveling acoustic modes, and, on the other hand, it gives access to a tailorable strong nonlinear gain and loss process in a small footprint that can lead to many new applications in nano- and microscale photonics (which will be further discussed in Sec. VI).

Forming a deeper understanding of the fundamental interactions between light and sound has drawn a lot of interest in recent years in the context of optomechanical cavities that aim to address fundamental scientific questions, for example, the observation of quantum effects in macroscopic systems.<sup>218–231</sup> With the focus on microscale SBS interactions, rather than long interaction lengths present in optical fibers, we now see a convergence of the fields of optomechanics and Brillouin scattering.<sup>232</sup> Inducing strong SBS in microscale waveguides requires careful consideration of the guidance mechanism of the optical, as well as the acoustic mode to ensure a strong mode overlap.<sup>233</sup> It also necessitates a deeper investigation of the optical forces involved in the generation of the acoustic waves, such as bulk electrostrictive forces, and their interplay with boundary forces, such as radiation pressure.<sup>27,138,234</sup>

The first demonstration of SBS in a micro-structured waveguide was achieved in photonic crystal fibers in 2006,<sup>44</sup> which were just

developed at that point.<sup>235,236</sup> Those fibers guide light by surrounding the fiber core with holes that provide spatial confinement of the optical mode in the transverse direction. The core of those fibers can be very small, which leads to a high concentration of optical energy (tight confinement) of the optical and acoustic waves and hence an enhancement of the Brillouin gain. Also, direct effects of the waveguide dimension on the measured Brillouin spectral response can be observed, and multiple spectral features were reported.<sup>44,237</sup> First, investigations of spectral features in the Brillouin response due to discrete phonon modes date back to the 1970s, when they were observed in thin films.<sup>238–243</sup>

Both types of Brillouin scattering, forward and backward, have been observed in the small core of photonic crystal fiber (forward Brillouin scattering is sometimes also referred to as Raman-like scattering due to its flat acoustic dispersion that resembles the shape of the dispersion curve for Raman scattering<sup>44</sup>). Building on those initial demonstrations more experimental and theoretical studies on Brillouin interactions in photonic crystal fibers followed.<sup>244–248</sup>

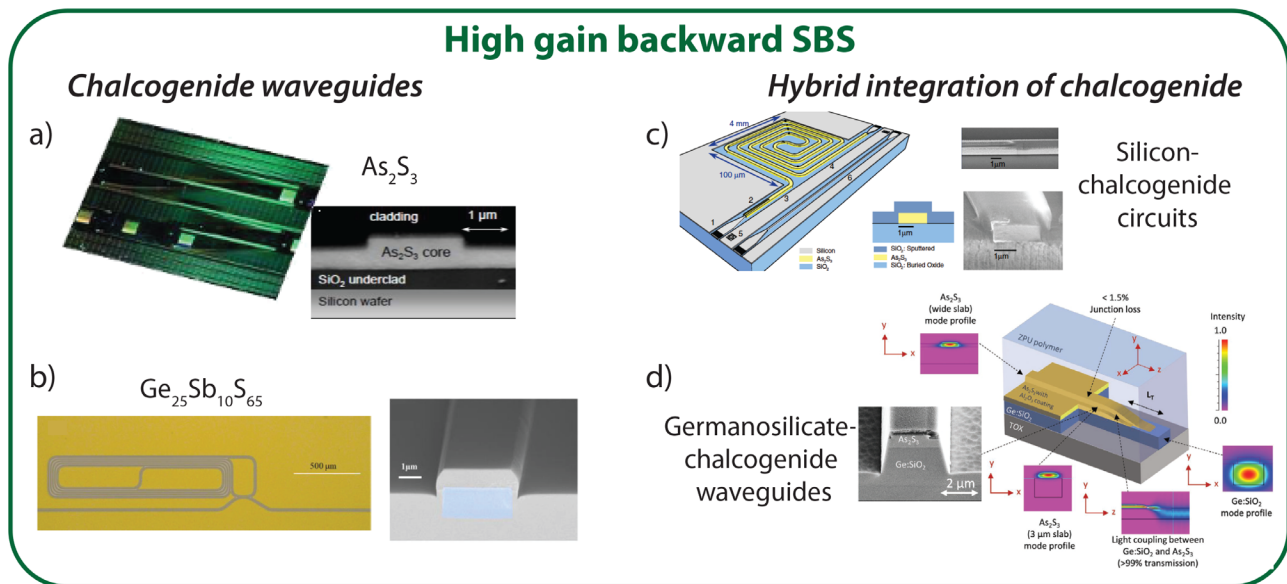
With the development of nanofabrication technologies and low-loss waveguides on a chip, the field of Brillouin scattering embraced the shift from fiber to integrated chip-scale platforms.<sup>3</sup> Two parallel trends for chip-scale platforms emerged: (1) SBS in high-Q resonators with precise control over the resonator dimension to enable SBS enhancement, and (2) low-loss on-chip waveguides that guide both optical and acoustic modes. In Secs. V A–V E, we provide an overview of the different on-chip waveguide architectures, as well as different material platforms for forward and backward SBS. In addition to more established platforms based on materials such as silicon and chalcogenide, we will also look at emerging waveguide materials and novel methods of actuating a Brillouin response on a chip, such as interdigitated transducer (IDT). An overview of the different platforms is shown in Figs. 6–9.

### A. SBS in chalcogenide waveguides

The first observation of large Brillouin gain in a planar waveguide on a chip was reported in 2011 by Pant *et al.*<sup>24</sup> in chalcogenide  $As_2S_3$  rib waveguides [photograph and scanning electron microscope image of the chip shown in Fig. 6(a)]. The waveguide had a cross-section of 4  $\mu\text{m}$  by 850 nm and a Brillouin frequency shift, linewidth, and gain of 7.7 GHz, 34 MHz, and 16 dB, respectively, were observed. To achieve large SBS gain on a length scale of cm to tens of cm, waveguides need to fulfill several requirements, such as low optical loss, small mode area, decent optical power handling without nonlinear losses, and, importantly, guidance of the optical and acoustic modes to ensure a large acousto-optic overlap.<sup>233</sup> To this end,  $As_2S_3$  waveguides are commonly surrounded by a silica cladding that ensures a larger optical refractive index in the core than the cladding but also a lower sound velocity and hence guidance of the acoustic mode via total internal reflection (in analogy to the optical mode case).<sup>233</sup>

The acoustic confinement is a key factor for achieving large SBS amplification, and gain values of up to 50 dB on a chip have been observed.<sup>249,250</sup> In contrast, directly laser-written chalcogenide waveguides only show small Brillouin gain values<sup>251</sup> which highlights again the importance of the acoustic guidance. In addition to the larger mode field diameter due to lower refractive index contrast, directly laser-written chalcogenide waveguides do not possess a large acoustic impedance mismatch between the core and the cladding, which leads





**FIG. 6.** Overview of different chip-based waveguide platforms that provide high gain backward SBS. (a) Chalcogenide  $\text{As}_2\text{S}_3$ <sup>24</sup> and (b)  $\text{Ge}_{25}\text{Sb}_{10}\text{S}_{65}$  waveguides.<sup>215</sup> (c) Hybrid integration of silicon and chalcogenide waveguides. A silicon taper ensures an efficient transition from silicon to chalcogenide.<sup>216</sup> (d) Chalcogenide rib waveguides on germanosilicate waveguides that are mode matched to the optical input fiber. The transition from germanosilicate to chalcogenide is achieved via a vertical taper.<sup>217</sup> (a) Reprinted with permission from Pant *et al.*, *Opt. Express* **19**, 8285–8290 (2011). Copyright 2011 The Optical Society.<sup>24</sup> (b) Reprinted with permission from Song *et al.*, *J. Lightwave Technol.* **39**, 5048–5053 (2021). Copyright 2021 IEEE.<sup>215</sup> (c) Reprinted with permission from Morrison *et al.*, *Optica* **4**, 847 (2017). Copyright 2017 The Optical Society.<sup>216</sup>

not only to low Brillouin gain but also a widened Stokes linewidth.<sup>251</sup> The observed linewidth of the Stokes wave is inversely proportional to the acoustic lifetime in the waveguide. Those results show that to achieve high Brillouin gain on a chip the core material and surrounding cladding material matter.

The largest reported on-chip SBS gain was in  $\text{As}_2\text{S}_3$  chalcogenide glass surrounded by silica, and hence the majority of on-chip applications that utilize SBS have been based on backward SBS in this waveguide architecture (see Sec. VI). Resonant enhancement of the Brillouin gain in those waveguides allowed cascading of the Brillouin process to many higher orders,<sup>137</sup> and it could have been shown that the cascaded Stokes waves are phase-locked.<sup>252</sup>

More recently SBS has been reported in other chalcogenide compositions, such as  $\text{Ge}_{25}\text{Sb}_{10}\text{S}_{65}$  [Fig. 6(b)].<sup>215</sup> The main motivation behind finding new chalcogenide compositions that support SBS is, on the one hand, to replace carcinogenic elements like Arsenic that need to be handled very carefully during the fabrication process, and, on the other hand, to increase the melting temperature of the softglass composite to enable chemical vapor deposition (CVD) of the silica cladding. Using CVD to deposit the silica cladding promises higher silica film quality and hence lower propagation loss. The reported Brillouin frequency shift, linewidth, and gain coefficient of  $\text{Ge}_{25}\text{Sb}_{10}\text{S}_{65}$  waveguides with silica cladding are 7.4 GHz, 48 MHz, and  $338 \text{ m}^{-1} \text{ W}^{-1}$ , respectively. The values are similar to what was achieved previously in  $\text{As}_2\text{S}_3$  but with a slightly lower SBS gain coefficient.

Whereas chalcogenide waveguides have the advantage of large Brillouin gain, they lack the availability of active components provided by standard manufacturing foundries based on silicon photonics. To

this end, hybrid integration of chalcogenide waveguides with silicon photonic circuits was proposed and demonstrated<sup>216</sup> to get the best of both worlds [Fig. 6(c)]. This early demonstration showed a transition from a silicon waveguide using a taper into a chalcogenide waveguide that provided more than 20 dB on-off gain and 18.5 dB net gain.

Another hybrid integration SBS platform that takes advantage of different material properties is chalcogenide glass on a germanosilicate film.<sup>217</sup> Here, light is coupled into germanosilicate and is then transferred to a chalcogenide waveguide via a vertical taper structure [Fig. 6(d)]. Germanosilicate waveguides are mode matched to the coupling fibers and hence improve coupling efficiency and, at the same time, greatly reduce back reflections from the pump laser at the facet of the chip. Due to the counter-propagating nature of the pump and the probe for backward SBS, those back reflections can cause distortions of the usually much weaker probe and often requires very narrowband filters.

## B. SBS in silicon

Silicon is an attractive material for photonic integration due to the existing infrastructure developed over decades for the integrated electronics industry. Hence, inducing SBS in silicon is enticing as it promises access to large-scale fabrication facilities and the most mature library of components offered by major semiconductor foundries. However, observing SBS in standard silicon-on-insulator (SOI) waveguides turned out to be challenging due to the high stiffness of silicon relative to the silica substrate, which means that the sound velocity in the silicon core is larger than in the surrounding substrate and the acoustic mode leaks away from the waveguide core.

A way to salvage SBS in silicon was proposed by Rakich and co-workers, who predicted theoretically strong SBS in suspended silicon waveguides with small cross sections via the interplay of bulk and boundary forces.<sup>234</sup> The combination of radiation pressure, electrostrictive bulk forces, and the high intensity due to the small effective area promises a giant enhancement of the Brillouin gain in those suspended silicon waveguides.

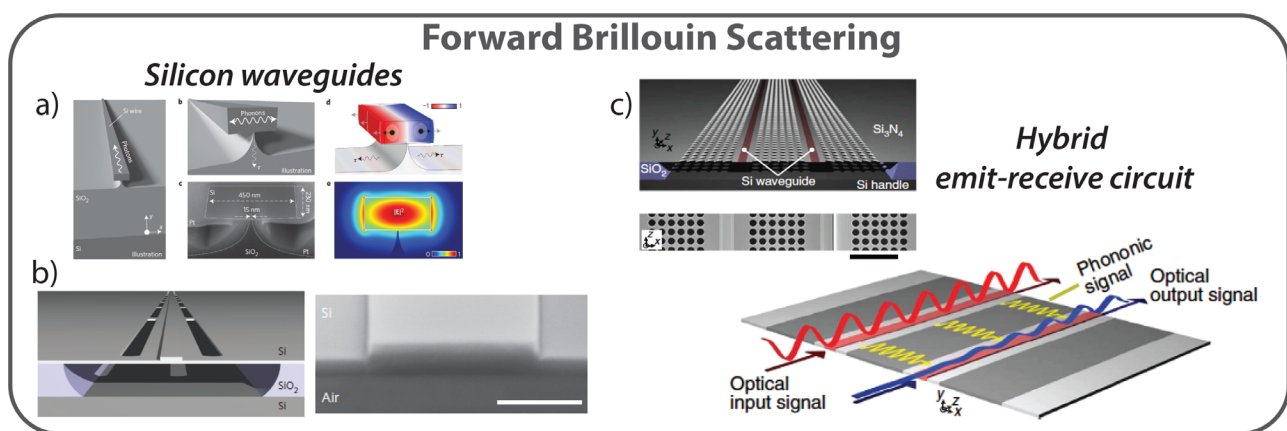
The challenge this theoretical finding posed to experimentalists was how to make a silicon waveguide that is removed from the substrate. In the wake of the theoretical predictions, many different approaches were pursued to suspend silicon waveguides from the underlying substrate (examples of suspended silicon structures that support SBS are shown in Figs. 7(a) and 7(b)). Broadly speaking, those silicon SBS waveguides are either supported by a thin pillar along their length<sup>27</sup> or supported laterally.<sup>253–256</sup>

The first demonstration of forward Brillouin scattering in silicon, however, was not shown in a simple suspended silicon nanowire as suggested by the theory but rather in a hybrid membrane structure made out of a suspended silicon waveguide that guides the optical mode, with silicon-nitride wings attached to the side to provide guidance to the acoustic mode and ensure a large overlap between the optical and acoustic mode in the waveguide core.<sup>255</sup> The forward Brillouin frequency shift could be tailored from 1 to 18 GHz in those waveguides and a Brillouin gain coefficient of around  $2570 \pm 540 \text{ W}^{-1} \text{ m}^{-1}$  could be observed.<sup>255</sup>

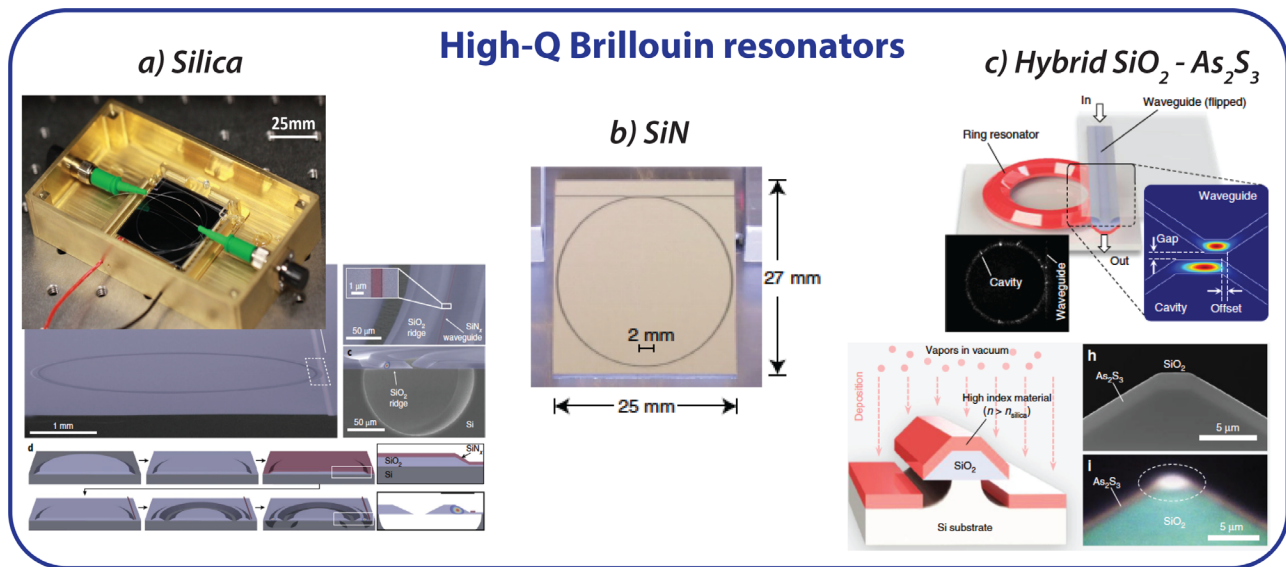
The first demonstration of forward Brillouin scattering in a suspended waveguide purely made of silicon followed shortly.<sup>27</sup> The structure consisted of silicon nanowires that were supported along their length by a several nm wide silica pillar. Suspending the waveguide greatly reduced leakage of the acoustic mode and it was shown that a narrower pillar structure leads to better confinement. The reported on-off gain in those silicon nanowires was around 0.6 dB despite a Brillouin gain coefficient of above  $3000 \text{ W}^{-1} \text{ m}^{-1}$ . The main limitation for the SBS on-off gain were nonlinear losses caused by two-photon absorption and free-carrier absorption that limited the coupled pump power to around 25 mW.<sup>27,257</sup>

After the initial demonstrations that forward Brillouin scattering can indeed be induced in silicon waveguides, major research efforts focused on increasing the achievable on-off gain with the target of achieving net amplification. To this end, different platforms were put forward and the first structure that achieved net gain, even though only a modest amount of 0.5 dB, was a series of  $25 \mu\text{m}$  long fully suspended silicon nanowires that were periodically supported by  $4.6 \mu\text{m}$  anchors.<sup>258</sup> The first silicon waveguide structure to achieve significant net gain of around 5 dB in silicon was a silicon rib waveguide on a suspended membrane [shown in Fig. 7(b)].<sup>253</sup> In addition to being fully made of silicon as opposed to the hybrid silicon–silicon nitride membrane described earlier, the cross-section of the rib waveguide was with a height of 210 nm, an etch depth of 80 nm, and a width of  $1 \mu\text{m}$  significantly larger than in previous demonstrations. The larger waveguide reduced the linear losses to below 0.2 dB/cm and significantly reduced the effects of nonlinear losses, which were a limiting factor in previous demonstrations in silicon.<sup>27,257,259</sup> A further increase in net gain was achieved by resonantly enhancing the Brillouin response.<sup>264</sup> Here, the silicon rib waveguide shown in Fig. 7(b) was wrapped into a racetrack resonator with two Brillouin active regions of around 7.5 mm length along the two parallel long sides of the elliptical racetrack. With this structure, net amplification exceeding 20 dB could be achieved.<sup>264</sup> A longer version of the racetrack resonator formed the basis of a Brillouin laser in silicon.<sup>265</sup> Other silicon structures that utilize resonant enhancement to achieve Brillouin gain in silicon are so-called bullseye optomechanical resonators.<sup>266</sup> The optical and acoustic modes are guided around the perimeter of the structure. Mechanical Bragg gratings that consist of concentric rings etched into the silicon membrane ensure guidance of the acoustic mode.

More recently, SBS research in silicon goes beyond the interaction of the fundamental optical mode in a single waveguide, and inter-modal interactions<sup>256</sup> as well as acoustic interactions across two waveguides [see Fig. 7(c)],<sup>254</sup> and a combination of both have been reported.<sup>267</sup> It was shown that in two silicon waveguides in close proximity connected via a patterned silicon nitride membrane, a transverse acoustic wave can modulate probe light in the other waveguide; this structure is referred to as photonic–phononic emitter–receiver



**FIG. 7.** Overview of different chip-based silicon platforms that support forward Brillouin scattering. (a) Suspended silicon waveguide on pillar.<sup>27</sup> (b) Suspended silicon rib waveguide.<sup>253</sup> (c) Hybrid photonic–phononic emitter–receiver structure [scanning electron microscope (SEM) image and conceptual diagram].<sup>254</sup> (a) Reprinted with permission from Van Laer *et al.*, *Nat. Photonics* **9**, 199–203 (2015). Copyright 2015 Springer Nature.<sup>27</sup> (b) Reprinted with permission from Kittlaus *et al.*, *Nat. Photonics* **10**, 463–467 (2016). Copyright 2016 Springer Nature.<sup>253</sup>



**FIG. 8.** Overview of different chip-based high-Q Brillouin resonators made out of (a) silica,<sup>260,261</sup> (b) SiN,<sup>262</sup> and (c) chalcogenide on silica.<sup>263</sup> [(a), top] Reprinted with permission from Lai *et al.*, *Nat. Photonics* **14**, 345 (2020). Copyright 2020 Springer Nature.<sup>260</sup> [(a), bottom] Reprinted with permission from Yang *et al.*, *Nat. Photonics* **12**, 297–302 (2018). Copyright 2018 Springer Nature.<sup>261</sup> (b) Reprinted with permission from Gundavarapu *et al.*, *Nat. Photonics* **13**, 60 (2018). Copyright 2020 Springer Nature.<sup>262</sup>

(PPER). The patterned silicon nitride membrane acts as a Bragg reflector for the acoustic wave and allows independent control of the optical and acoustic mode and the acoustic coupling between two waveguides.<sup>254</sup> A monolithic silicon version of this PPER was later shown as the basis of RF filters<sup>268</sup> and two silicon rib waveguides without the Bragg patterning formed the basis of an on-chip isolator.<sup>267</sup> In addition to the PPER structure, the isolator also relied on Brillouin-induced mode conversion from the fundamental to a higher order optical mode. Inter-modal Brillouin scattering itself was achieved just prior in a single suspended silicon rib waveguide combined with integrated mode multiplexers.<sup>256</sup>

### C. SBS in high-Q resonators

As we have seen in Secs. VA and VB, the Brillouin response can be significantly enhanced in a resonator structure. In this section, we discuss different high-Q resonator structures that support SBS, focusing on structures that are integrated on a chip. As the Brillouin frequency shift is in the GHz to tens of GHz and its narrow linewidth in the MHz to tens of MHz, fabricating a resonator with the matching free spectral range (FSR) posed a major challenge.

The first demonstration of SBS in a high-Q resonator was reported in 2009 in a  $CaF_2$  resonator where the FSR was matched to the Brillouin frequency shift.<sup>23</sup> The loaded Q-factor of the resonator was around  $4 \times 10^9$  which enabled Brillouin lasing with a threshold as low as  $3 \mu\text{W}$ . Shortly after this initial demonstration, SBS was observed in small silica fiber tip resonators with a diameter of around  $100 \mu\text{m}$  by exploiting higher order optical modes.<sup>269</sup>

The first demonstration of SBS in a resonator fabricated on a chip using nano-lithography techniques was reported in a silica wedge resonator in 2012 that had a Q-factor of  $875 \times 10^6$ .<sup>270</sup> This platform was further developed to increase compatibility with scalable fabrication techniques and ease of coupling into the resonator, and a new

design that includes a SiN bus waveguide was put forward and experimentally demonstrated<sup>261</sup> [see Fig. 8(a)].

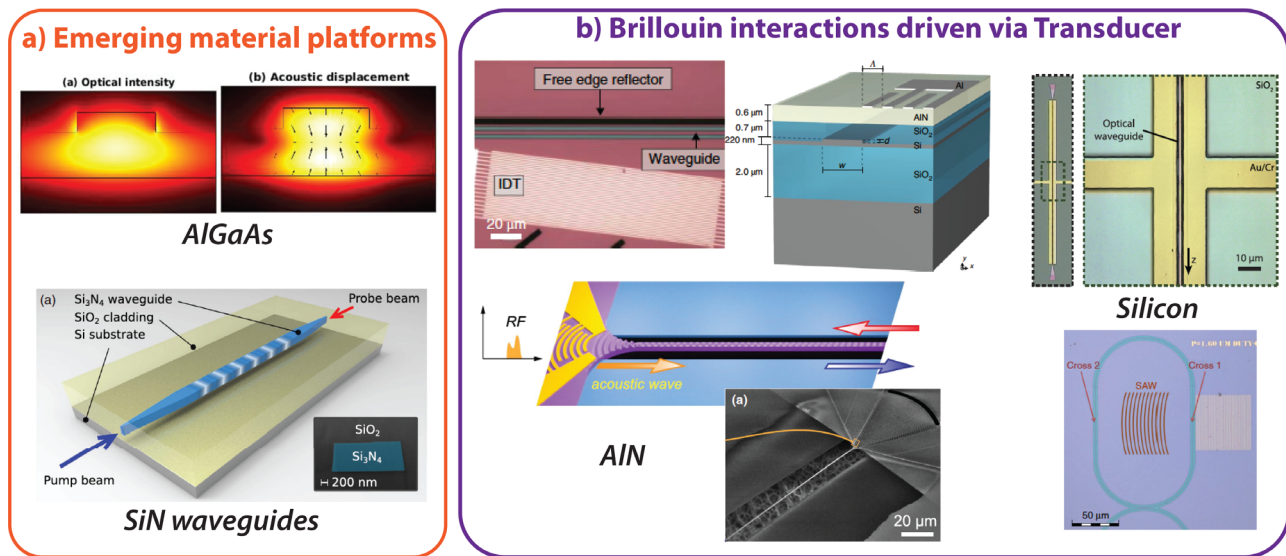
In addition to high-Q resonators made of silica, other materials have been explored that can provide high-Q, and hence, a low Brillouin threshold integrated on a chip. One material that shows a lot of promise due to its low loss is silicon nitride  $Si_3N_4$ <sup>262</sup> [see Fig. 8(b)]. Interestingly, the acoustic mode in this structure is not well guided. The observed Brillouin shift of 10.93 GHz is determined by the silica that surrounds the  $Si_3N_4$  and the observed Brillouin gain bandwidth of 153 MHz attests to the leaky nature of the acoustic wave. However, due to the high loaded optical Q-factor of  $28 \times 10^6$ , Brillouin lasing was observed for around 10 mW on-chip optical pump power and laser linewidths below a Hertz have been measured.

The resonator structures discussed so far were using materials like silica and  $Si_3N_4$  that provide very low optical loss but have not necessarily the largest Brillouin gain coefficient. In the case of the  $Si_3N_4$  resonator, the acoustic wave is not even very well guided. Another approach that was recently demonstrated forms a resonator of highly nonlinear materials like chalcogenide glass  $As_2S_3$ <sup>263</sup> [see Fig. 8(c)]. The main challenge here is to reduce the propagation loss of the chalcogenide waveguide, usually caused by sidewall roughness induced in the etching process. The solution proposed and demonstrated in Ref. 263 is depositing chalcogenide glass on top of a trapezoid silica waveguide ring. Using this technique, a Q-factor of  $1.44 \times 10^7$  and a Brillouin laser threshold of 0.53 mW could have been demonstrated.

### D. Emerging material platforms

Recently, the field has seen the emergence of new waveguide materials for on-chip SBS that go beyond the so far discussed chalcogenide glasses and silicon waveguides that might provide optical amplification, very low waveguides losses, or even larger Brillouin gain coefficients. One exciting material is silicon nitride, as it offers ultra-





**FIG. 9.** (a) Emerging material platforms for Brillouin scattering such as AlGaAs<sup>273</sup> and SiN waveguides,<sup>271</sup> and (b) alternative approaches to excite acoustic waves on a chip in AIN<sup>274–276</sup> or silicon.<sup>277,278</sup> [(a), top] From Jin *et al.*, *Conference on Lasers and Electro-Optics*. Copyright 2020 The Optical Society. Reprinted with permission from Optical Society.<sup>273</sup> [(b), bottom left] Reprinted with permission from Liu *et al.*, *Optica* **6**, 778 (2019). Copyright 2019 The Optical Society.<sup>276</sup> [(b), top right] Reprinted with permission from Van Laer *et al.*, *APL Photonics* **3**, 086102 (2018). Copyright 2018 AIP Publishing LLC.<sup>277</sup> [(b), top left] Reprinted with permission from Sohn *et al.*, *Nat. Photonics* **12**, 91–97 (2018). Copyright 2018 Springer Nature.<sup>274</sup> [(b), top center] Reprinted with permission from Otterstrom *et al.*, *Science* **360**, 1113–1116 (2018). Copyright 2018 American Association for the Advancement of Science.<sup>267</sup> (b) Reprinted with permission from Kittlaus *et al.*, *Nat. Photonics* **15**, 43–52 (2021). Copyright 2020 Springer Nature.<sup>275</sup>

low propagation loss and wideband transparency that includes the visible range (405–2350 nm).<sup>262</sup> As seen for high-Q silicon nitride resonators, the acoustic mode is not guided when the waveguide core is surrounded by silica and only the large optical Q-factor of those resonators allowed the observation of Brillouin lasing despite the short-lived acoustic wave.<sup>262</sup> Nevertheless, the first report of Brillouin scattering in a single-pass optical waveguide made out of silicon nitride in a silica matrix was reported in 2020 [see schematic of waveguide in Fig. 9(a)].<sup>271</sup> Not surprisingly, the leakage of the acoustic mode in the architecture led to a very low gain coefficient of just  $0.07 \text{ m}^{-1} \text{ W}^{-1}$ . Recent attempts to improve the SBS gain in silicon nitride aimed to improve the guidance of the acoustic wave in a silica layer between two silicon nitride stripe waveguides. A tailorable Brillouin gain coefficient between 0.12 and  $0.29 \text{ m}^{-1} \text{ W}^{-1}$  depending on the waveguide width could have been observed in this case.<sup>272</sup>

A second promising platform for SBS that is yet in its infancy is AlGaAs.<sup>273</sup> High modal confinement, low propagation loss, and compatibility with other III-V gain materials are all attractive attributes and motivate the further exploration of this material composition. Importantly, in contrast to many other semiconductor platforms, it promises acoustic confinement when on a silica substrate [modeling of the optical and acoustic mode in AlGaAs are shown in Fig. 9(a)]. The first demonstration of SBS in a non-suspended AlGaAs waveguide was reported recently; however, the experimentally achieved gain is yet under 1 dB (Ref. 273) and further engineering and investigation are required to make it a feasible platform for SBS.

### E. Brillouin interactions driven via transducers

Finally, we want to discuss another method to induce SBS in chip-scale waveguides that uses IDTs instead of optically driving the

acoustic wave via electrostriction.<sup>274–278</sup> The interaction of the wave with an optical probe still occurs via the photoelastic effect like in traditionally optically pumped systems and the interaction needs to fulfill the phase-matching condition between traveling acoustic and optical waves. However, not relying on an optical pump enables inducing of strong acoustic fields, which can be an advantage, particularly in platforms that suffer from nonlinear losses such as two-photon absorption that limit the available pump power. We note that the transducer-based approach has a close resemblance to traditional acousto-optic modulation schemes. Acousto-optic modulators are quite mature devices that usually operate in the MHz regime. As we had seen a convergence of optomechanics and Brillouin scattering when the field moved to tailored on-chip waveguides, we can see similar trends for the research fields of acousto-optics, surface acoustic waves (SAWs), and Brillouin scattering.

Figure 9(b) shows a racetrack waveguide on a suspended membrane made out of AIN with an Al IDT at an angle next to it.<sup>274</sup> AIN is a piezoelectric material, and the IDTs are driven via an RF tone that induces acoustic waves that travel across the racetrack waveguides. The acoustic waves induce mode conversion of the optical mode in the waveguide, which leads to non-reciprocal modulation over a 1 GHz bandwidth. The non-reciprocal bandwidth was later extended to more than 100 GHz by utilizing an AIN membrane with Al IDTs on top of a silicon waveguide.<sup>275</sup> The third demonstration of electromechanically driven acoustic waves in AIN showed high-frequency 16 GHz acoustic waves traveling along a suspended waveguide.<sup>276</sup>

In addition to the above examples of electromechanically induced Brillouin scattering in AIN, it has been shown that mechanical waves can be induced in silicon via transducer.<sup>277,278</sup> It was demonstrated that



7.2 GHz mechanical waves can be excited in a suspended silicon waveguide via capacitive coupling,<sup>277</sup> see Fig. 9(b). Another approach to induce mechanical waves in an SOI platform is based on the thermoelastic expansion of metal gratings hit by a pump laser.<sup>278</sup> This generates a surface acoustic wave at up to 8 GHz that travels across a silicon race-track waveguide where it interacts with the optical probe. The advantage of this approach is that it works in a standard SOI platform without the need to underetch.

VI. APPLICATIONS OF ON-CHIP SBS

Since the first demonstration of on-chip SBS, a multitude of applications have been shown in the laboratory harnessing different

material platforms, waveguide types, and resonator structures. An overview of a selection of applications is shown in Figs. 10 and 11. Broadly speaking, on-chip applications can be categorized into integrated optical signal manipulation, generation, and processing or integrated microwave photonic signal processing and generation.<sup>3,279–281</sup>

A. SBS for integrated microwave photonic signal processing

SBS is a very attractive effect for integrated microwave photonics due to its narrow linewidth, tunability, reconfigurability, and ability to provide gain or loss in a small form factor. Not surprisingly, SBS was

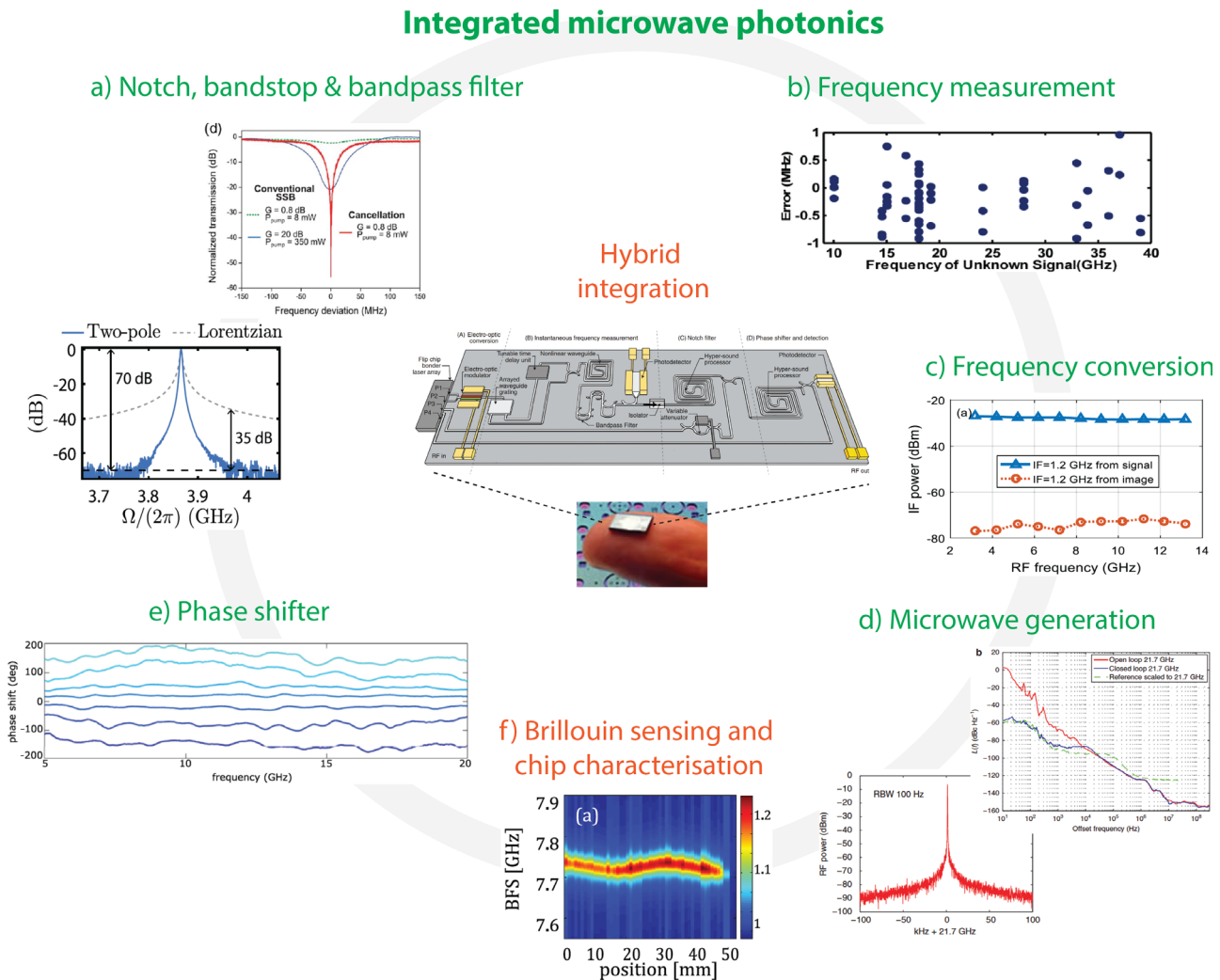


FIG. 10. Overview of different MWP applications utilizing on-chip SBS. (a) Notch<sup>282</sup> and bandpass filter;<sup>286</sup> (b) high-precision frequency measurement;<sup>283</sup> (c) broadband frequency conversion with image rejection;<sup>284</sup> (d) generation of stable, low-phase noise microwave signals;<sup>285</sup> high-resolution on-chip Brillouin sensing;<sup>161</sup> (e) wideband phase-shifter;<sup>286</sup> center: image of photonic chip with artist's impression of fully integrated hybrid Brillouin circuit.<sup>3</sup> [(a), bottom and (f)] Reprinted with permission from Gertler *et al.*, APL Photonics 5, 096103 (2020). Copyright 2020 AIP Publishing LLC.<sup>288</sup> [(a) top] Reprinted with permission from Marpaung *et al.*, Optica 2, 76 (2015). Copyright 2015 The Optical Society.<sup>282</sup> (b) Reprinted with permission from Jiang *et al.*, Optica 3, 30 (2016). Copyright 2016 The Optical Society.<sup>283</sup> (c) Reprinted with permission from Zhu *et al.*, Opt. Lett. 45, 5571 (2020). Copyright 2020 The Optical Society.<sup>284</sup> (e) Reprinted with permission from McKay *et al.*, Optica 6, 907 (2019).<sup>286</sup> Copyright 2019 The Optical Society.

demonstrated in a multitude of applications in MWP, ranging from filtering, frequency measurement to phase-shifters and microwave sources. In general, those applications harness the narrowband amplitude response to filter optical signals and/or utilize the narrowband and optically tunable phase shift induced by the SBS resonance to manipulate the phase of a signal or induce a time delay.

The most straightforward way to harness on-chip SBS in a microwave photonic link is to induce a filter profile based on either the SBS loss (gain) on the optical sideband, which upon photodetection leads to a narrow stop band (passband)—given by the Brillouin linewidth—in the RF domain. Such a filter scheme has been implemented in a chalcogenide rib waveguide utilizing 20 dB gain of the sideband amplitude induced by SBS to generate a 23 MHz wide filter and tunability of the center frequency from 2 to 12 GHz.<sup>287</sup> Those metrics exemplify some of the key advantages SBS brings to MWP signal processing, namely, the high resolution and frequency tunability. However, using SBS directly to amplify one sideband requires quite a lot of pump power to get decent filter rejection, which is challenging due to the short effective length, power handling of the chips, and insertion loss from the facet, which increases the overall power consumption. Over time, more sophisticated schemes have been developed to overcome that issue by using interference between different optical sidebands combined with SBS to achieve deeper filter rejection [see Fig. 10(a), top].<sup>282</sup> Following those initial demonstrations of an MWP filter based on backward SBS in chalcogenide waveguides, many further papers followed that improved different aspects of the filter, such as bandwidth tuning of the pass and stopbands, number of stop and passbands, insertion loss, noise figure, and linearity with an overview given in Ref. 288.

Whereas it is fair to say that most microwave photonic filter applications of on-chip SBS are currently based on backward SBS in chalcogenide waveguides, filter functions have also been implemented using forward Brillouin scattering in silicon.<sup>268,289</sup> An example of a microwave photonic filter in a silicon waveguide is shown in Fig. 10(a), bottom. Here, a bandpass filter with a steep roll-off in PPER silicon waveguides has been demonstrated.<sup>268</sup> Due to the nature of the PPER structure, the pump and the probe are in individual waveguides, and hence, the need for on-chip circulators or a narrowband filter to separate the pump and probe is alleviated.

Filters are fundamental building blocks of many systems and the SBS filter technology described above formed the basis for further functionalities, such as, for example, frequency mixing and frequency measurement,<sup>283,284</sup> Fig. 10. It was shown that the steep amplitude response of an SBS-based filter induced in chalcogenide waveguides can be used to perform amplitude-to-frequency mapping via the filter transfer function and extract the frequency of an unknown RF signal over a wide bandwidth with errors as small as 1 MHz,<sup>283</sup> see Fig. 10(b).

Frequency conversion and mixing are indispensable in any microwave system as it converts the carrier frequency to a frequency within the bandwidth of the analog-to-digital converter (ADC) and digital-to-analog converter (DAC). An optical mixer will harness an optical local oscillator that beats with the optical signal of interest at a photodetector that generates the desired frequency-converted signal via heterodyning. Harnessing on-chip SBS, a frequency mixer was demonstrated that converts signals over a 10 GHz bandwidth to an intermediate frequency of 1.2 GHz with a conversion gain of  $-9$  dB

and, importantly, around 50 dB of image rejection [Fig. 10(c)].<sup>284</sup> Image signals are located symmetrically around the local oscillator, and during the frequency conversion would fall into the same band as the signal of interest and cause distortions that cannot anymore be removed by filtering.

For frequency mixers and many other microwave applications, stable oscillators are essential. It has been shown that on-chip high-Q resonators with the FSR matched to the Brillouin frequency shift can be used to synthesize ultra-stable microwave signals,<sup>285</sup> see Fig. 10(d). The first- and third-order Stokes waves generated in the resonator are beating at the photodetector, creating a beat tone at 21.7 GHz with an open loop phase noise of  $-110$  dBc/Hz at 100 kHz. Another method to synthesize stable microwave signals based on integrated photonics is the OEO, where the mode selecting filter function can be induced via SBS on a chip.<sup>290</sup> Again SBS offers wide tunability as the filter function can be moved via altering the optical pump wavelength. Beyond signal generation, it has been shown that the on-chip OEO can also be used to identify frequency signals that are fed into the OEO cavity and lead to stable oscillations above the OEO threshold that can be detected at the OEO output.<sup>291</sup>

Another important device required in microwave systems is phase shifter or delay lines, which enable, for example, beam steering in phase arrayed antennas (PAAs). Here, chip integration is crucial to fit the signal processing at the element level, which is given by half the wavelength of the signal.<sup>292</sup> Using this method, Brillouin-based phase shifters have been shown in chalcogenide rib waveguides.<sup>249,293</sup> A continuously tunable phase shift over  $240^\circ$  from 1.5 to 31 GHz with only 1.5 dB of amplitude fluctuations has been shown in a chip-based demonstration.<sup>293</sup>

While phase shifters enable beam steering in PAAs for signals with a large bandwidth, they can induce beam squint, essentially a distortion of the beam pattern as different frequencies are deflected by a different angle. To overcome this limitation, true-time delay systems can be utilized to perform the beam steering function. In MWP, a true-time delay can be achieved by controlling the phase of the optical carrier while inducing a time delay of the sideband, a technique known as separate carrier tuning.<sup>294</sup> As we have seen, SBS is predestined for implementing such a system as it can induce a narrowband phase shift on the optical carrier as well as a delay of the sideband via Brillouin slow-light.<sup>96,97</sup> Such a system was shown utilizing on-chip SBS and achieving a  $200^\circ$  phase shift and a 4 ns delay over 100 MHz using 52 dB of on-off SBS gain.<sup>249</sup>

As these demonstrations exemplify, SBS offers great potential for phase shifting and delaying signals; however, large Brillouin gain and hence large pump powers are required to achieve a full  $360^\circ$  phase shift. To this end, interference schemes that can enhance the phase shift induced via on-chip SBS have been put forward.<sup>286,295,296</sup> Two RF tones, transduced in the optical domain, beating on a photodetector add vectorially and small phase shifts can be enhanced. Using this technique, it has been shown that even a modest amount of Brillouin ( $<2$  dB) generated by forward Brillouin scattering in a suspended silicon waveguide could be enhanced to a full  $360^\circ$  over a bandwidth of 15 GHz [Fig. 10(e)].<sup>286</sup> This phase enhancement scheme has also been shown for a true-time delay system that combined SBS gain in chalcogenide waveguides with SiN ring resonators.<sup>296</sup>

Brillouin sensing techniques described earlier in this paper can play a crucial role in the photonic integration process. Traditionally

utilized in long length of fiber, recent work has shown on-chip distributed sensing with sub-mm resolution that can be used to characterize the waveguide uniformity and the localized SBS gain in the circuit [Fig. 10(f)].<sup>161,297,298</sup> Both are important parameters for the evaluation, design, and optimization of photonic integrated circuits.

## B. SBS for integrated optical signal processing and generation

We have seen in Sec. VI A the benefits of SBS for microwave photonic signal processing in a small form factor, and the application space for optical signal processing, controlling, manipulation, and generation is equally wide and diverse (see Fig. 11). In the optical domain, additional properties of SBS, such as the phase matching condition, are used to achieve functionalities like non-reciprocity and optical isolation,<sup>267</sup> nonlinear mode conversion,<sup>256</sup> delay and storage of optical signals induced by coupling to slowly moving sound waves,<sup>300</sup> or ultra-narrowband lasing in resonators.<sup>262</sup> This section provides an overview of different chip-based applications harnessing SBS.

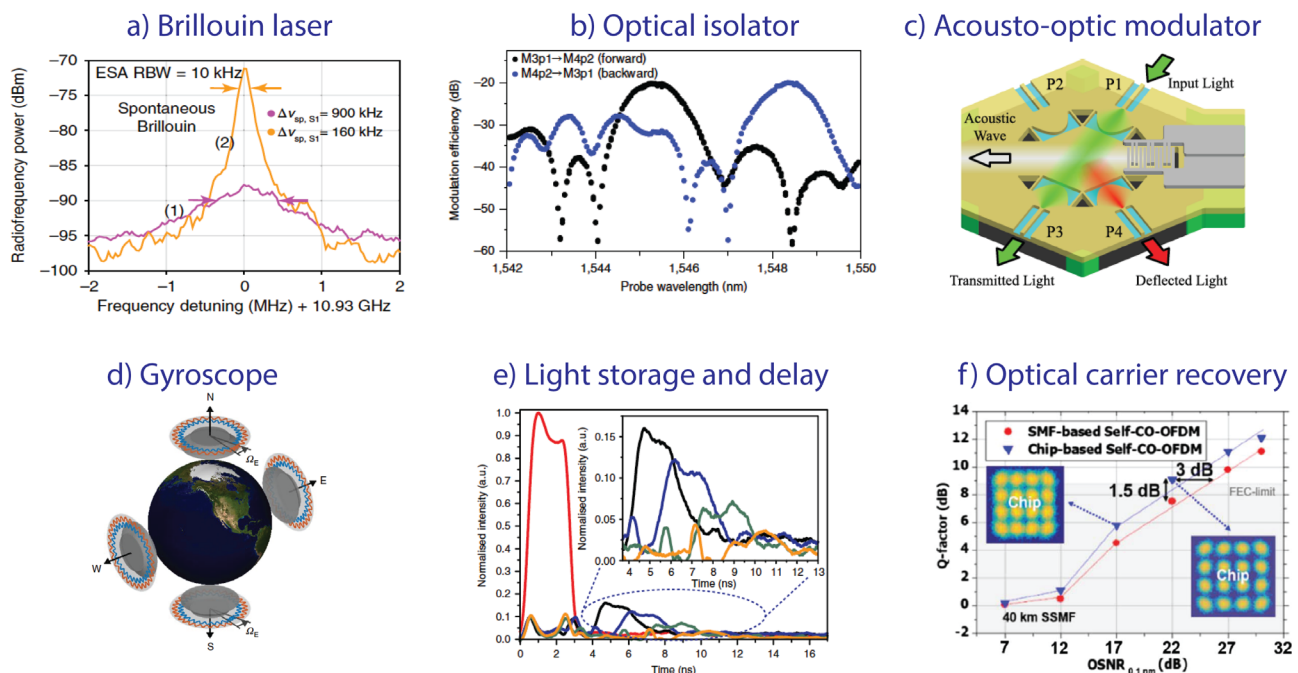
One critical component for future fully integrated photonics circuits is pure and stable laser sources integrated on the chip. Brillouin lasers offer a way to overcome current bottlenecks as they allow to significantly narrow the linewidth of their pump laser that drives the Brillouin oscillation. This linewidth narrowing occurs when the decay

rate of the acoustic wave in the resonator is faster than the optical loss rate. In this scenario, the generated Stokes wave will experience Schawlow-Townes linewidth narrowing above the laser threshold.<sup>301,302</sup>

In particular, improvements in nanofabrication techniques enabled a rapid increase in optical Q-factor achievable on-chip that led to lower threshold Brillouin lasers with linewidths reaching the sub-hertz level [Fig. 11(a)].<sup>262</sup> The operation wavelength of Brillouin lasers is determined by the wavelength of the pump laser and the transparency window of the waveguide/resonator, which gives it enormous flexibility and an extension of the wavelength range of on-chip Brillouin laser into the visible wavelength range has been reported.<sup>303</sup> In addition to generating narrow linewidth laser signals on a chip, Brillouin lasers in high-Q resonators have been used as gyroscopes [Fig. 11(d)].<sup>260</sup> Here, two counter-propagating Stokes waves are generated in a resonator using two Brillouin pumps and the Sagnac shift is measured. The sensitivity of the Brillouin laser gyroscope was good enough to measure the rotation of the earth.<sup>260</sup>

Another highly desired on-chip component readily available in optical fiber systems is the optical isolators. Optical isolators are essential to avoid backpropagation of the laser through the circuit and form the basis for circulators to route counterpropagating signals. Here, Brillouin scattering offers an elegant and powerful way to achieve non-reciprocity. The basic underlying principle of Brillouin-based isolators,

## Integrated optical applications and signal processing



**FIG. 11.** Overview of different optical signal processing applications utilizing on-chip SBS. (a)–(c) shows critical components for integrated circuits, such as lasers,<sup>262</sup> isolators,<sup>267</sup> and modulators.<sup>299</sup> Panel (d) highlights an application of on-chip Brillouin scattering for rotation sensing,<sup>260</sup> while (e) and (f) show to examples of optical signal processing, that is, all-optical delays<sup>300</sup> and optical carrier recovery.<sup>144</sup> (a) Reprinted with permission from Gundavarapu *et al.* Nat. Photonics 13, 60 (2018). Copyright 2018 Springer Nature.<sup>262</sup> (b) Reprinted with permission from Kittlaus *et al.*, Nat. Photonics 12, 613–620 (2018). Copyright 2018 Springer Nature.<sup>267</sup> (c) Reprinted with permission from Li *et al.*, APL Photonics 4, 080802 (2019). Copyright 2019 AIP Publishing LLC.<sup>299</sup> (d) Reprinted with permission from Lai *et al.*, Nat. Photonics 14, 345 (2020). Copyright 2020 Springer Nature.<sup>260</sup> (f) Reprinted with permission from Giacomidis *et al.*, Optica 5, 1191 (2018). Copyright 2018 The Optical Society.<sup>144</sup>

or non-reciprocity more generally, are transitions between optical modes via acoustic waves. The phase-matching condition of the Brillouin process assures that only modes traveling in a certain direction can undergo mode conversion but not signals traveling in the opposite direction, as first theoretically proposed by Huang and Fan.<sup>304</sup> Different ways have been put forward to induce acoustic mode conversion on chip, like optically pumped PPER silicon waveguide structures<sup>267</sup> [a measured non-reciprocal spectrum is shown in Fig. 11(b)], multimode silicon racetrack resonator,<sup>264</sup> or electrically driven acoustic waves.<sup>274,275</sup> Using Brillouin scattering, large operation bandwidths exceeding 100 GHz and 38 dB non-reciprocal contrast could have been achieved.<sup>267</sup>

Photonic integrated circuits have low transit times; hence, methods to delay or buffer signals are required for many applications. Following the initial fiber demonstrations,<sup>96,97</sup> Brillouin slow-light has been shown on a photonic chip.<sup>305</sup> Despite the larger Brillouin gain coefficient, the delay and time-bandwidth product faced the same limitations as the fiber implementation. However, a different delay scheme, that is, Brillouin light storage, greatly benefited from the higher local Brillouin gain available on the chip [multiple delayed optical signals are shown in Fig. 11(e)].<sup>300</sup> Record fractional delays could be achieved, and Brillouin effects with optical pulses in the 100 ps regime could be investigated<sup>306</sup> and recent efforts to counteract the decay of the acoustic wave via optical pumping promises storage times even beyond the intrinsic acoustic lifetime.<sup>307</sup> It was shown that not only the amplitude information but also the phase information is maintained in the storage and retrieval process.<sup>300</sup> Furthermore, the phase matching condition allows the storage of wavelength division multiplexed signals in a single waveguide without cross-talk<sup>308</sup> and nonreciprocal delays.<sup>309</sup>

For optical communication applications, such as optical carrier recovering via narrowband SBS amplification, chip integration promises not only a great reduction in SWAP-C but also increased polarization and phase stability compared to fiber-based solutions [Fig. 11(f)].<sup>144</sup> Self-coherent communication systems do not require an LO; however, they usually require a large guard band around the carrier to be able to filter it. Using on-chip SBS, it could be shown that the guard bandwidth can be reduced to approximately 265 MHz for signal rates of up to 116.82 Gbit/s.<sup>144</sup>

As described in the MWP section, many optical signal processing applications will greatly benefit from further integration of components on a single chip (highlighted by the illustration in the middle of Fig. 10), such as, for example, all-integrated gyroscopes. However, while microwave photonic applications always require a full circuit, that is, MWP link, that includes an EO-modulator and photodetector, some of the applications described in this section are rather individual building blocks of a bigger circuit, such as laser sources, isolators, or delay lines. One additional building block of next-generation photonic integrated circuits is shown in Fig. 10(c).<sup>299</sup> This Brillouin-based acousto-optic modulator has great potential to route, switch, or modulate optical signals.<sup>299</sup>

## VII. FUTURE PERSPECTIVE—CHALLENGES AND OPPORTUNITIES

We have reviewed the progress in science and applications of Brillouin light scattering over the past 100 years to date. Here, we look

at what is next for Brillouin scattering science and technology and identify the main themes for future developments and discovery.

Stemming from the theme of Brillouin scattering on a chip, discussed extensively in Secs. V and VI of this review, integration and miniaturization will continue to remain an important direction for researchers around the world in order to create smaller and more energy-efficient devices and systems as well as speed up the translation of research discoveries to industry. This will incorporate the search for new or improved materials and novel waveguide designs that allow tailoring of the Brillouin gain as well as photon and phonon dispersion profiles and ensure high opto-acoustic overlap for energy-efficient transfer between optical and acoustic modes. Further efforts in tailoring phonon dissipation and guiding mechanisms will be required to improve the performance of novel platforms like SiN, and creative solutions are required like, for example, anti-resonant acoustic guidance.<sup>310</sup>

In a similar way, methods to achieve guidance in SOI waveguides without underetching would increase compatibility with standard silicon photonic circuits, like the theoretical proposal of geometrically softened mechanical modes in fin-like structures.<sup>311</sup> Interestingly, this theoretical study also suggests the possibility of inducing strong backward SBS in silicon, which is yet elusive. The main underlying reason for the absence of backward SBS in silicon is the weaker  $p_{12}$  component of the photoelastic tensor, which couples the transverse electromagnetic fields to the longitudinal acoustic wave, compared to silica and other materials. Being able to induce backward SBS in silicon via carefully designed waveguide geometries would open the door to many applications in microwave photonics and optical signal processing currently limited to chalcogenide waveguides.

Inducing large Brillouin gain in direct bandgap materials like AlGaAs would open many new opportunities for applications that require optical gain. Nevertheless, the focus will remain on understanding constraints and removing those for SBS interactions in silicon, the material platform preferred for technology translation and device mass production due to the abundance of resources and standardized infrastructure already existent in this area. Despite many efforts, photonic integration is still in its infancy, with many opportunities available for combining building blocks of SBS systems on one chip-scale platform, including driving lasers, Brillouin gain media, modulators, filters, and detectors. When it comes to Brillouin microscopy and imaging, the work on photonic integration has only started with first demonstrations of Brillouin fiber probes reported in the last 5 years.<sup>312,313</sup> Harnessing evanescent field coupling to Brillouin modes using nano-waveguides offers new ways for sensing the surroundings and microscopy.<sup>314</sup>

In addition to further progress in integrated photonic waveguides designs and integration of Brillouin-active waveguides with other on-chip components, there are novel demonstrations of Brillouin scattering in optical fibers. For example, Brillouin scattering has been shown in chiral photonic crystal fiber,<sup>315</sup> gas-filled fibers,<sup>32</sup> and liquid core fibers.<sup>316</sup> Furthermore, Brillouin scattering was recently evanescently induced at the surrounding of nanofibers, which marks an important step in connecting waveguide technology with Brillouin sensing and spectroscopy applications, as well as bare signal amplification in a small footprint.<sup>314</sup> It remains to be seen if experiments that are currently demonstrated in optical fiber will inspire on-chip implementations in the future as we have seen in the past.



Quantum technology has been a blossoming field of research with powerful ideas being disseminated to other areas of physics, engineering, chemistry, and biology. On the one hand, the quantum regime has been hugely unexplored in the context of Brillouin lasing, memory, and signal processing using opto-acoustic interactions characteristic of Brillouin light scattering. Many fundamental questions still remain on the nature of these interactions at a single phonon level that are worth investigating. Recent reports of Brillouin scattering reaching the strong coupling regime in high-Q resonators are an important step toward quantum Brillouin applications.<sup>317</sup> Investigations of Brillouin scattering in a quantum regime at very low temperatures have a lot of unexplored potential, and the first reports of Brillouin lasing in superfluids have just emerged.<sup>318</sup> Exploring the possibilities to harness the Brillouin gain or loss to explore non-Hermitian physics and exceptional points is another research direction that can lead to novel applications and offer deeper insight into some fundamental physics.<sup>319</sup> On the other hand, quantum technologies such as quantum control of the states of light, known as squeezed light, can add benefits to overall system performance by pushing optical detection to levels beyond shot noise. This direction is especially attractive for the Brillouin imaging community since it allows to perform microscopy at reduced power levels over extended periods of time without incurring photodamage to biological samples.

The future will also see more emphasis on numerical processing techniques, complementing and, more importantly, overcoming the shortcomings of hardware and instrumentation limitations. Machine learning algorithms directed to optimize the time required for the acquisition of images in Brillouin microscopy or to retrieve more information from hyper-spectral data are many examples where numerical signal processing will play a crucial role in the dissemination of the technology as a routine imaging modality for micro-mechanical mapping in a broad range of scenarios from industrial material sensing to medical imaging and disease diagnostics. Beyond imaging, it is anticipated that machine learning will play a growing role in Brillouin research. Be it to find new waveguide designs with large Brillouin gain or to enhance the precision of microwave photonic frequency measurements or distributed Brillouin sensors. For example, it has been shown that genetic optimization codes can improve the performance of distributed Brillouin fiber sensors.<sup>187</sup>

We have shown in this review how a prediction of coupling light to acoustic waves 100 years ago spawned an active and diverse research community that covers biological applications and microscopy, distributed sensing over many kilometers, and advanced signal processing applications in optical fibers as well as integrated photonic circuits. Despite being a diverse community, we see invigoration of ideas across the different domains of Brillouin scattering research and we can see a bright and exciting future for the field for more fundamental science discoveries and a maturing of many of the technological applications toward real-world impact and opening new regimes of fundamental physics, for example, quantum properties. With all the progress in the last 100 years of research on Brillouin scattering, we can only imagine what the next 100 years will bring.

## ACKNOWLEDGMENTS

We acknowledge the ARC Grant Nos. DP190100992, DP200101893, DP220101431, and DP190101973 and fruitful ongoing

collaboration with Professor Michael Steel, Professor Chris Poulton, and Professor Steve Madden.

## AUTHOR DECLARATIONS

### Conflict of Interest

The authors have no conflicts to disclose.

### Author Contributions

**Moritz Merklein:** Writing – original draft (lead). **Irina Kabakova:** Writing – original draft (equal); Writing – review & editing (equal). **Atiyeh Zarifi:** Writing – original draft (supporting); Writing – review & editing (supporting). **Benjamin J. Eggleton:** Conceptualization (equal); Supervision (equal); Writing – original draft (supporting); Writing – review & editing (supporting).

## DATA AVAILABILITY

Data sharing is not applicable to this article as no new data were created or analyzed in this study.

## REFERENCES

- <sup>1</sup>L. Brillouin, "Diffusion de la lumière et des Rayons X par un corps transparent homogène," *Ann. Phys.* **9**, 88–122 (1922).
- <sup>2</sup>A. Kobayakov, M. Sauer, and D. Chowdhury, "Stimulated Brillouin scattering in optical fibers," *Adv. Opt. Photonics* **2**, 1–59 (2010).
- <sup>3</sup>B. J. Eggleton, C. G. Poulton, P. T. Rakich, M. J. Steel, and G. Bahl, "Brillouin integrated photonics," *Nat. Photonics* **13**, 664 (2019).
- <sup>4</sup>G. Scarcelli and S. H. Yun, "Confocal Brillouin microscopy for three-dimensional mechanical imaging," *Nat. Photonics* **2**, 39–43 (2008).
- <sup>5</sup>C. A. Galindez-Jamioy and J. M. López-Higuera, "Brillouin distributed fiber sensors: An overview and applications," *J. Sens.* **2012**, 204121.
- <sup>6</sup>L. Thévenaz, "Brillouin distributed time-domain sensing in optical fibers: State of the art and perspectives," *Front. Optoelectron. China* **3**, 13–21 (2010).
- <sup>7</sup>X. Bao and L. Chen, "Recent progress in Brillouin scattering based fiber sensors," *Sensors* **11**, 4152–4187 (2011).
- <sup>8</sup>E. Gross, "Change of wave-length of light due to elastic heat waves at scattering in liquids," *Nature* **126**, 201–202 (1930).
- <sup>9</sup>C. V. Raman and C. S. Venkateswaran, "Optical observation of the Debye heat waves in crystals," *Nature* **142**, 250–250 (1938).
- <sup>10</sup>R. S. Krishnan, "Elastic constant of crystals from light scattering measurements," *Proc. Indian Acad. Sci., Sect. A* **41**, 91–97 (1954).
- <sup>11</sup>R. Chiao, C. Townes, and B. Stoicheff, "Stimulated Brillouin scattering and coherent generation of intense hypersonic waves," *Phys. Rev. Lett.* **12**, 592–595 (1964).
- <sup>12</sup>E. Garmire and C. H. Townes, "Stimulated Brillouin scattering in liquids. I," *Appl. Phys. Lett.* **5**, 84 (1964).
- <sup>13</sup>R. Brewer and K. Rieckhoff, "Stimulated Brillouin scattering in liquids," *Phys. Rev. Lett.* **13**, 334–336 (1964).
- <sup>14</sup>E. E. Hagenlocker and W. G. Rado, "Stimulated Brillouin and Raman scattering in gases," *Appl. Phys. Lett.* **7**, 236 (1965).
- <sup>15</sup>E. Ippen and R. Stolen, "Stimulated Brillouin scattering in optical fibers," *Appl. Phys. Lett.* **21**, 539 (1972).
- <sup>16</sup>K. O. Hill, B. S. Kawasaki, and D. C. Johnson, "CW Brillouin laser," *Appl. Phys. Lett.* **28**, 608 (1976).
- <sup>17</sup>J. R. Sandercock, "Simple stabilization scheme for maintenance of mirror alignment in a scanning February–Perot interferometer," *J. Phys. E: Sci. Instrum.* **9**, 566–569 (1976).
- <sup>18</sup>D. Culverhouse, F. Farahi, C. Pannell, and D. Jackson, "Potential of stimulated Brillouin scattering as sensing mechanism for distributed temperature sensors," *Electron. Lett.* **25**, 913 (1989).

- <sup>19</sup>M. Shirasaki, "Large angular dispersion by a virtually imaged phased array and its application to a wavelength demultiplexer," *Opt. Lett.* **21**, 366 (1996).
- <sup>20</sup>M. Nikles, L. Thevenaz, and P. A. Robert, "Brillouin gain spectrum characterisation in single-mode optical fibers," *IEEE J. Lightwave Technol.* **15**, 1842–1851 (1997).
- <sup>21</sup>P. Dainese, P. S. J. Russell, N. Joly, J. C. Knight, G. S. Wiederhecker, H. L. Fragnito, V. Laude, and A. Khelif, "Stimulated Brillouin scattering from multi-GHz-guided acoustic phonons in nanostructured photonic crystal fibers," *Nat. Phys.* **2**, 388–392 (2006).
- <sup>22</sup>K. Y. Song, W. Zou, Z. He, and K. Hotate, "All-optical dynamic grating generation based on Brillouin scattering in polarization-maintaining fiber," *Opt. Lett.* **33**, 926 (2008).
- <sup>23</sup>I. S. Grudin, A. B. Matsko, and L. Maleki, "Brillouin lasing with a CaF<sub>2</sub> whispering gallery mode resonator," *Phys. Rev. Lett.* **102**, 043902 (2009).
- <sup>24</sup>R. Pant, C. G. Poulton, D.-Y. Choi, H. Mcfarlane, S. Hile, E. Li, L. Thevenaz, B. Luther-Davies, S. J. Madden, and B. J. Eggleton, "On-chip stimulated Brillouin scattering," *Opt. Express* **19**, 8285–8290 (2011).
- <sup>25</sup>T. Deschamps, J. Margueritat, C. Martinet, A. Mermet, and B. Champagnon, "Elastic moduli of permanently densified silica glasses," *Sci. Rep.* **4**, 7193 (2014).
- <sup>26</sup>C. W. Ballmann, J. V. Thompson, A. J. Traverso, Z. Meng, M. O. Scully, and V. V. Yakovlev, "Stimulated Brillouin scattering microscopic imaging," *Sci. Rep.* **5**, 18139 (2015).
- <sup>27</sup>R. Van Laer, B. Kuyken, D. Van Thourhout, and R. Baets, "Interaction between light and highly confined hypersound in a silicon photonic nanowire," *Nat. Photonics* **9**, 199–203 (2015).
- <sup>28</sup>A. Létoublon, S. Paofai, B. Rufflé, P. Bourges, B. Hehlen, T. Michel, C. Ecolivet, O. Durand, S. Cordier, C. Katan, and J. Even, "Elastic constants, optical phonons, and molecular relaxations in the high temperature plastic phase of the CH<sub>3</sub>NH<sub>3</sub>PbBr<sub>3</sub> hybrid perovskite," *J. Phys. Chem. Lett.* **7**, 3776–3784 (2016).
- <sup>29</sup>V. E. Gusev and P. Ruelo, "Advances in applications of time-domain Brillouin scattering for nanoscale imaging," *Appl. Phys. Rev.* **5**, 031101 (2018).
- <sup>30</sup>C. W. Ballmann, Z. Meng, A. J. Traverso, M. O. Scully, and V. V. Yakovlev, "Impulsive Brillouin microscopy," *Optica* **4**, 124 (2017).
- <sup>31</sup>I. Remer, R. Shaashoua, N. Shemesh, A. Ben-Zvi, and A. Bilencu, "High-sensitivity and high-specificity biomechanical imaging by stimulated Brillouin scattering microscopy," *Nat. Methods* **17**, 913–916 (2020).
- <sup>32</sup>F. Yang, F. Gyger, and L. Thévenaz, "Intense Brillouin amplification in gas using hollow-core waveguides," *Nat. Photonics* **14**, 700–708 (2020).
- <sup>33</sup>S. Shahrokhi, M. Dubajic, Z. Z. Dai, S. Bhattacharyya, R. A. Mole, K. C. Rule, M. Bhadbhade, R. Tian, N. Mussakhanuly, X. Guan, Y. Yin, M. P. Nielsen, L. Hu, C. H. Lin, S. L. Chang, D. Wang, I. V. Kabakova, G. Conibeer, S. Bremner, X. G. Li, C. Cazorla, and T. Wu, "Anomalous structural evolution and glassy lattice in mixed-halide hybrid perovskites," *Small* **18**, 2200847 (2022).
- <sup>34</sup>C. Poon, J. Chou, M. Cortie, and I. Kabakova, "Brillouin imaging for studies of micromechanics in biology and biomedicine: From current state-of-the-art to future clinical translation," *J. Phys. Photonics* **3**, 012002 (2021).
- <sup>35</sup>A. R. Chraplyvy, "Limitations on Lightwave communications imposed by optical-fiber nonlinearities," *J. Lightwave Technol.* **8**, 1548–1557 (1990).
- <sup>36</sup>L. Mandelstam, "Light scattering by inhomogeneous media," *Zh. Russ. Fiz-Khim* **58**, 381 (1926).
- <sup>37</sup>R. W. Boyd, *Nonlinear Optics* (Academic Press, 2003).
- <sup>38</sup>C. V. Raman and K. S. Krishnan, "The optical analogue of the Compton effect," *Nature* **121**, 711–711 (1928).
- <sup>39</sup>C. V. Raman and K. S. Krishnan, "The negative absorption of radiation," *Nature* **122**, 12–13 (1928).
- <sup>40</sup>C. V. Raman, "A change of wave-length in light scattering," *Nature* **121**, 619–619 (1928).
- <sup>41</sup>P. Debye and F. W. Sears, "On the scattering of light by supersonic waves," *Proc. Natl. Acad. Sci. U. S. A.* **18**, 409–414 (1932).
- <sup>42</sup>C. V. Raman and N. S. N. Nathe, "The diffraction of light by high frequency sound waves. I," *Proc. Indian Acad. Sci., Sect. A* **2**, 406–412 (1935).
- <sup>43</sup>E. L. Feinberg, "Igor' Evgen'evich Tamm," *Phys.-Usp.* **38**, 773–789 (1995).
- <sup>44</sup>P. Dainese, P. S. J. Russell, G. S. Wiederhecker, N. Joly, H. L. Fragnito, V. Laude, and A. Khelif, "Raman-like light scattering from acoustic phonons in photonic crystal fiber," *Opt. Express* **14**, 4141–4150 (2006).
- <sup>45</sup>I. V. Kabakova, I. Azuri, Z. Chen, P. K. Nayak, H. J. Snait, L. Kronik, C. Paterson, A. A. Bakulin, and D. A. Egger, "The effect of ionic composition on acoustic phonon speeds in hybrid perovskites from Brillouin spectroscopy and density functional theory," *J. Mater. Chem. C* **6**, 3861–3868 (2018).
- <sup>46</sup>T. H. Maiman, "Stimulated optical radiation in ruby," *Nature* **187**, 493–494 (1960).
- <sup>47</sup>E. Garmire, "Perspectives on stimulated Brillouin scattering," *New J. Phys.* **19**, 011003 (2017).
- <sup>48</sup>R. Y. Chiao and B. P. Stoicheff, "Brillouin scattering in liquids excited by the He-Ne maser," *J. Opt. Soc. Am.* **54**, 1286 (1964).
- <sup>49</sup>N. M. Kroll, "Excitation of hypersonic vibrations by means of photoelastic coupling of high-intensity light waves to elastic waves," *J. Appl. Phys.* **36**, 34–43 (1965).
- <sup>50</sup>C. L. Tang, "Saturation and spectral characteristics of the Stokes emission in the stimulated Brillouin process," *J. Appl. Phys.* **37**, 2945–2955 (1966).
- <sup>51</sup>D. Pohl, M. Maier, and W. Kaiser, "Phonon lifetimes measured in amplifiers for Brillouin radiation," *Phys. Rev. Lett.* **20**, 366–368 (1968).
- <sup>52</sup>P. J. Wu, I. V. Kabakova, J. W. Ruberti, J. M. Sherwood, I. E. Dunlop, C. Paterson, P. Török, and D. R. Overby, "Water content, not stiffness, dominates Brillouin spectroscopy measurements in hydrated materials," *Nat. Methods* **15**, 561–562 (2018).
- <sup>53</sup>G. Scarcelli, W. J. Polacheck, H. T. Nia, K. Patel, A. J. Grodzinsky, R. D. Kamm, and S. H. Yun, "Noncontact three-dimensional mapping of intracellular hydromechanical properties by Brillouin microscopy," *Nat. Methods* **12**, 1132–1134 (2015).
- <sup>54</sup>F. Palombo, C. P. Winlove, R. S. Edginton, E. Green, N. Stone, S. Caponi, M. Madami, and D. Fioretto, "Biomechanics of fibrous proteins of the extracellular matrix studied by Brillouin scattering," *J. R. Soc. Interface* **11**, 20140739 (2014).
- <sup>55</sup>F. Palombo and D. Fioretto, "Brillouin light scattering: Applications in biomedical sciences," *Chem. Rev.* **119**, 7833 (2019).
- <sup>56</sup>A. C. Ferreira, A. Létoublon, S. Paofai, S. Raymond, C. Ecolivet, B. Rufflé, S. Cordier, C. Katan, M. I. Saidaminov, A. A. Zhumekenov, O. M. Bakr, J. Even, and P. Bourges, "Elastic softness of hybrid lead halide perovskites," *Phys. Rev. Lett.* **121**, 085502 (2018).
- <sup>57</sup>R. Raghunathan, J. Zhang, C. Wu, J. Rippey, M. Singh, K. Larin, and G. Scarcelli, "Evaluating biomechanical properties of murine embryos using Brillouin microscopy and optical coherence tomography," *J. Biomed. Opt.* **22**(8), 086013 (2017).
- <sup>58</sup>C. Bevilacqua, H. Sánchez-Iranzo, D. Richter, A. D.-M. noz, and R. Prevedel, "Imaging mechanical properties of sub-micron ECM in live zebrafish using Brillouin microscopy," *Biomed. Opt. Express* **10**, 1420–1431 (2019).
- <sup>59</sup>G. Antonacci, R. M. Pedrigi, A. Kondiboyina, V. V. Mehta, R. de Silva, C. Paterson, R. Krams, and P. Török, "Quantification of plaque stiffness by Brillouin microscopy in experimental thin cap fibroatheroma," *J. R. Soc. Interface* **12**, 20150843 (2015).
- <sup>60</sup>P. Shao, T. G. Seiler, A. M. Eltony, A. Ramier, S. J. J. Kwok, G. Scarcelli, R. P. II, and S.-H. Yun, "Effects of corneal hydration on Brillouin microscopy in vivo effect of corneal hydration on Brillouin frequency," *Invest. Ophthalmol. Visual Sci.* **59**, 3020–3027 (2018).
- <sup>61</sup>M. Matsukawa, R. Tsubota, M. Kawabe, and K. Fukui, "Application of a micro-Brillouin scattering technique to characterize bone in the GHz range," *Ultrasonics* **54**, 1155–1161 (2014).
- <sup>62</sup>F. Palombo, M. Madami, N. Stone, and D. Fioretto, "Mechanical mapping with chemical specificity by confocal Brillouin and Raman microscopy," *Analyst* **139**, 729–733 (2014).
- <sup>63</sup>A. Karampatzakis, C. Z. Song, L. P. Allsopp, A. Filloux, S. A. Rice, Y. Cohen, T. Wohland, and P. Torok, "Probing the internal micromechanical properties of pseudomonas aeruginosa biofilms by Brillouin imaging," *npj Biofilms Microbiomes* **3**, 20 (2017).
- <sup>64</sup>J. Margueritat, A. Virgone-Carlotta, S. Monnier, H. Delanoë-Ayari, H. C. Mertani, A. Berthelot, Q. Martinet, X. Dagany, C. Rivière, J.-P. Rieu, and T. Dehoux, "High-frequency mechanical properties of tumors measured by Brillouin light scattering," *Phys. Rev. Lett.* **122**, 018101 (2019).

- <sup>65</sup>C. Conrad, K. Gray, K. Stroka, I. Rizvi, and G. Scarcelli, "Mechanical characterization of 3D ovarian cancer nodules using Brillouin confocal microscopy," *Cell. Mol. Bioeng.* **12**, 215–226 (2019).
- <sup>66</sup>M. Troyanova-Wood, Z. Meng, and V. V. Yakovlev, "Differentiating melanoma and healthy tissues based on elasticity-specific Brillouin microspectroscopy," *Biomed. Opt. Express* **10**, 1774–1781 (2019).
- <sup>67</sup>J. Zhang, A. Fiore, S.-H. Yun, H. Kim, and G. Scarcelli, "Line-scanning Brillouin microscopy for rapid non-invasive mechanical imaging," *Sci. Rep.* **6**, 35398 (2016).
- <sup>68</sup>G. Antonacci and S. Braakman, "Biomechanics of subcellular structures by non-invasive Brillouin microscopy," *Sci. Rep.* **6**, 37217 (2016).
- <sup>69</sup>W. E. Moerner, "Single-molecule mountains yield nanoscale cell images," *Nat. Methods* **3**, 781–782 (2006).
- <sup>70</sup>K. I. Willig, R. R. Kellner, R. Medda, B. Hein, S. Jakobs, and S. W. Hell, "Nanoscale resolution in GFP-based microscopy," *Nat. Methods* **3**, 721–723 (2006).
- <sup>71</sup>P. S. Shen, "The 2017 Nobel prize in chemistry: Cryo-EM comes of age," *Anal. Bioanal. Chem.* **410**, 2053–2057 (2018).
- <sup>72</sup>K. J. Koski and J. L. Yarger, "Brillouin imaging," *Appl. Phys. Lett.* **87**, 061903 (2005).
- <sup>73</sup>J. R. Sandercock, "Brillouin-scattering measurements on silicon and germanium," *Phys. Rev. Lett.* **28**, 237–240 (1972).
- <sup>74</sup>G. Scarcelli, P. Kim, and S. H. Yun, "In vivo measurement of age-related stiffening in the crystalline lens by Brillouin optical microscopy," *Biophys. J.* **101**, 1539–1545 (2011).
- <sup>75</sup>G. Scarcelli and S. H. Yun, "In vivo Brillouin optical microscopy of the human eye," *Opt. Express* **20**, 9197 (2012).
- <sup>76</sup>I. Remer and A. Bilenca, "High-speed stimulated Brillouin scattering spectroscopy at 780 nm," *APL Photonics* **1**, 061301 (2016).
- <sup>77</sup>C. A. Casacio, L. S. Madsen, A. Terrasson, M. Waleed, K. Barnscheidt, B. Hage, M. A. Taylor, and W. P. Bowen, "Quantum-enhanced nonlinear microscopy," *Nature* **594**, 201–206 (2021).
- <sup>78</sup>H. Yuan, P. Zhang, and F. Gao, "Compressive hyperspectral Raman imaging via randomly interleaved scattering projection," *Optica* **8**, 1462–1470 (2021).
- <sup>79</sup>X. S. Yao, "High-quality microwave signal generation by use of Brillouin scattering in optical fibers," *Opt. Lett.* **22**, 1329–1331 (1997).
- <sup>80</sup>A. Loayssa, D. Benito, and M. J. Garde, "Optical carrier Brillouin processing of microwave photonic signals," *Opt. Lett.* **25**, 1234–1236 (2000).
- <sup>81</sup>J. Domingo, J. Pelayo, F. Villuendas, C. Heras, and E. Pellejer, "Very high resolution optical spectrometry by stimulated Brillouin scattering," *IEEE Photonics Technol. Lett.* **17**, 855–857 (2005).
- <sup>82</sup>K. Kao and G. Hockham, "Dielectric-fibre surface waveguides for optical frequencies," *Proc. Inst. Electr. Eng.* **113**, 1151 (1966).
- <sup>83</sup>R. G. Smith, "Optical power handling capacity of low loss optical fibers as determined by stimulated Raman and Brillouin Scattering," *Appl. Opt.* **11**, 2489 (1972).
- <sup>84</sup>R. W. Boyd, K. Rzaewski, and P. Narum, "Noise initiation of stimulated Brillouin scattering," *Phys. Rev. A* **42**, 5514 (1990).
- <sup>85</sup>K. O. Hill, D. C. Johnson, and B. S. Kawasaki, "CW generation of multiple Stokes and anti-Stokes Brillouin-shifted frequencies," *Appl. Phys. Lett.* **29**, 185–187 (1976).
- <sup>86</sup>L. F. Stokes, M. Chodorow, and H. J. Shaw, "All-fiber stimulated Brillouin ring laser with submilliwatt pump threshold," *Opt. Lett.* **7**, 509–511 (1982).
- <sup>87</sup>N. A. Olsson and J. P. Van Der Ziel, "Characteristics of a semiconductor laser pumped Brillouin amplifier with electronically controlled bandwidth," *J. Lightwave Technol.* **5**, 147–153 (1987).
- <sup>88</sup>E. Lichtman, R. Waarts, and A. Friesem, "Stimulated Brillouin scattering excited by a modulated pump wave in single-mode fibers," *J. Lightwave Technol.* **7**, 171–174 (1989).
- <sup>89</sup>A. Gaeta and R. Boyd, "Stimulated Brillouin scattering in the presence of external feedback," *Int. J. Nonlinear Opt. Phys. Mater.* **1**, 581–594 (1992).
- <sup>90</sup>C. G. Atkins, D. Cotter, D. W. Smith, and R. Wyatt, "Application of Brillouin amplification in coherent optical transmission," *Electron. Lett.* **22**, 556–558 (1986).
- <sup>91</sup>A. R. Chraplyvy and R. W. Tkach, "Narrowband tunable optical filter for channel selection in densely packed WDM systems," in *Optical Fiber Communication* (Optical Society of America, Washington, DC, 1987), Vol. 1100, p. WJ2.
- <sup>92</sup>T. Tanemura, Y. Takushima, and K. Kikuchi, "Narrowband optical filter, with a variable transmission spectrum, using stimulated Brillouin scattering in optical fiber," *Opt. Lett.* **27**, 1552 (2002).
- <sup>93</sup>B. Vidal, M. A. Piqueras, and J. Martí, "Tunable and reconfigurable photonic microwave filter based on stimulated Brillouin scattering," *Opt. Lett.* **32**, 23 (2007).
- <sup>94</sup>W. Zhang and R. A. Minasian, "Widely tunable single-passband microwave photonic filter based on stimulated Brillouin scattering," *IEEE Photonics Technol. Lett.* **23**, 1775–1777 (2011).
- <sup>95</sup>W. Zhang and R. A. Minasian, "Ultrawide tunable microwave photonic notch filter based on stimulated Brillouin scattering," *IEEE Photonics Technol. Lett.* **24**, 1182–1184 (2012).
- <sup>96</sup>K. Y. Song, M. Herráez, and L. Thévenaz, "Observation of pulse delaying and advancement in optical fibers using stimulated Brillouin scattering," *Opt. Express* **13**, 82–88 (2005).
- <sup>97</sup>Y. Okawachi, M. Bigelow, J. Sharping, Z. Zhu, A. Schweinsberg, D. Gauthier, R. Boyd, and A. Gaeta, "Tunable all-optical delays via Brillouin slow light in an optical fiber," *Phys. Rev. Lett.* **94**, 153902 (2005).
- <sup>98</sup>Z. Zhu, D. J. Gauthier, and R. W. Boyd, "Stored light in an optical fiber via stimulated Brillouin scattering," *Science* **318**, 1748–1750 (2007).
- <sup>99</sup>A. Loayssa and F. J. Lahoz, "Broad-band RF photonic phase shifter based on stimulated Brillouin scattering and single-sideband modulation," *IEEE Photonics Technol. Lett.* **18**, 208–210 (2006).
- <sup>100</sup>V. J. Urlick, K. J. Williams, and J. D. McKinney, *Fundamentals of Microwave Photonics* (John Wiley & Sons, 2015).
- <sup>101</sup>Y. Shen, X. Zhang, and K. Chen, "All-optical generation of microwave and millimeter wave using a two-frequency Bragg grating-based Brillouin fiber laser," *J. Lightwave Technol.* **23**, 1860–1865 (2005).
- <sup>102</sup>Y. G. Shee, M. A. Mahdi, M. H. Al-Mansoori, S. Yaakob, R. Mohamed, A. K. Zamzuri, A. Man, A. Ismail, and S. Hitam, "All-optical generation of a 21 GHz microwave carrier by incorporating a double-Brillouin frequency shifter," *Opt. Lett.* **35**, 1461 (2010).
- <sup>103</sup>J. Liu, L. Zhan, P. Xiao, G. Wang, L. Zhang, X. Liu, J. Peng, and Q. Shen, "Generation of step-tunable microwave signal using a multiwavelength Brillouin fiber laser," *IEEE Photonics Technol. Lett.* **25**, 220–223 (2013).
- <sup>104</sup>S. Preußler, N. Wenzel, R.-P. Braun, N. Owschmikow, C. Vogel, A. Deninger, A. Zadok, U. Woggon, and T. Schneider, "Generation of ultra-narrow, stable and tunable millimeter- and terahertz- waves with very low phase noise," *Opt. Express* **21**, 23950–23962 (2013).
- <sup>105</sup>J. B. Khurgin, "Performance limits on delay lines based on optical amplifiers," *Opt. Lett.* **31**, 948–950 (2006).
- <sup>106</sup>M. González-Herráez, S. Martín-Lopez, and L. Thévenaz, "Analytical expression of pulse broadening in an arbitrary linear slow light medium," *Opt. Lett.* **37**, 3171–3173 (2012).
- <sup>107</sup>L. Zhang, M. A. Soto, and L. Thévenaz, "Minimizing distortion and enlarging group delay in Brillouin slow light systems by gain profile optimization," in *Asia Communications and Photonics Conference* (Optical Society of America, 2014), Vol. 1, p. ATH2C.4.
- <sup>108</sup>S. Preussler, K. Jamshidi, A. Wiatrek, R. Henker, C.-A. Bunge, and T. Schneider, "Quasi-light-storage based on time-frequency coherence," *Opt. Express* **17**, 15790–15798 (2009).
- <sup>109</sup>T. Schneider, K. Jamshidi, and S. Preussler, "Quasi-light storage: A method for the tunable storage of optical packets with a potential delay-bandwidth product of several thousand bits," *J. Lightwave Technol.* **28**, 2586–2592 (2010).
- <sup>110</sup>S. Preussler, A. Wiatrek, K. Jamshidi, and T. Schneider, "Quasi-light-storage enhancement by reducing the Brillouin gain bandwidth," *Appl. Opt.* **50**, 4252–4256 (2011).
- <sup>111</sup>K. Y. Song, K. Lee, and S. B. Lee, "Tunable optical delays based on Brillouin dynamic grating in optical fibers," *Opt. Express* **17**, 10344–10349 (2009).
- <sup>112</sup>S. Chin and L. Thévenaz, "Tunable photonic delay lines in optical fibers," *Laser Photonics Rev.* **6**, 724–738 (2012).
- <sup>113</sup>Y. Antman, L. Yaron, T. Langer, M. Tur, N. Levanon, and A. Zadok, "Experimental demonstration of localized Brillouin gratings with low off-peak



- reflectivity established by perfect Golomb codes," *Opt. Lett.* **38**, 4701–4704 (2013).
- <sup>114</sup>R. Stolen, "Polarization effects in fiber Raman and Brillouin lasers," *IEEE J. Quantum Electron.* **15**, 1157–1160 (1979).
- <sup>115</sup>T. Horiguchi, N. Shibata, Y. Azuma, and M. Tateda, "Brillouin gain variation due to a polarization-state change of the pump or Stokes fields in standard single-mode fibers," *Opt. Lett.* **14**, 329 (1989).
- <sup>116</sup>M. van Deventer and A. Boot, "Polarization properties of stimulated Brillouin scattering in single-mode fibers," *J. Lightwave Technol.* **12**, 585–590 (1994).
- <sup>117</sup>A. Küng, L. Thévenaz, and P. A. Robert, "Polarization analysis of Brillouin scattering in a circularly birefringent fiber ring resonator," *J. Lightwave Technol.* **15**, 977–981 (1997).
- <sup>118</sup>S. Randoux and J. Zemmouri, "Polarization dynamics of a Brillouin fiber ring laser," *Phys. Rev. A* **59**, 1644–1653 (1999).
- <sup>119</sup>A. Zadok, E. Zilka, A. Eyal, L. Thévenaz, and M. Tur, "Vector analysis of stimulated Brillouin scattering amplification in standard single-mode fibers," *Opt. Express* **16**, 21692 (2008).
- <sup>120</sup>D. Samaniego and B. Vidal, "Brillouin wavelength-selective all-optical polarization conversion," *Photonics Res.* **8**, 440–447 (2020).
- <sup>121</sup>A. Wise, M. Tur, and A. Zadok, "Sharp tunable optical filters based on the polarization attributes of stimulated Brillouin scattering," *Opt. Express* **19**, 21945 (2011).
- <sup>122</sup>S. Preussler, A. Zadok, A. Wiatrek, M. Tur, and T. Schneider, "Enhancement of spectral resolution and optical rejection ratio of Brillouin optical spectral analysis using polarization pulling," *Opt. Express* **20**, 14734 (2012).
- <sup>123</sup>S. Preussler and T. Schneider, "Attometer resolution spectral analysis based on polarization pulling assisted Brillouin scattering merged with heterodyne detection," *Opt. Express* **23**, 26879 (2015).
- <sup>124</sup>Aragon Photonics, *Product Brochure: T&M Equipment Optical Communications* (Aragon Photonics, 2021).
- <sup>125</sup>Y. Dong, T. Jiang, L. Teng, H. Zhang, L. Chen, X. Bao, and Z. Lu, "Sub-MHz ultrahigh-resolution optical spectrometry based on Brillouin dynamic gratings," *Opt. Lett.* **39**, 2967 (2014).
- <sup>126</sup>N. Choksi, Y. Liu, R. Ghasemi, and L. Qian, "Sub-megahertz spectral dip in a resonator-free twisted gain medium," *Nat. Photonics* **16**, 498 (2022).
- <sup>127</sup>S. S. A. A., B. Yelkar, and R. Pant, "Analogue of electromagnetically induced absorption in the microwave domain using stimulated Brillouin scattering," *Commun. Phys.* **3**, 109 (2020).
- <sup>128</sup>D. A. Fishman and J. A. Nagel, "Degradations due to stimulated Brillouin scattering in multigigabit intensity-modulated fiber-optic systems," *J. Lightwave Technol.* **11**, 1721–1728 (1993).
- <sup>129</sup>K. Shiraki, M. Ohashi, and M. Tateda, "Suppression of stimulated Brillouin scattering in a fibre by changing the core radius," *Electron. Lett.* **31**, 668 (1995).
- <sup>130</sup>K. Shiraki, M. Ohashi, and M. Tateda, "Performance of strain-free stimulated Brillouin scattering suppression fiber," *J. Lightwave Technol.* **14**, 549–554 (1996).
- <sup>131</sup>N. A. Brilliant, "Stimulated Brillouin scattering in a dual-clad fiber amplifier," *J. Opt. Soc. Am. B* **19**, 2551–2557 (2002).
- <sup>132</sup>A. F. El-Sherif and T. A. King, "High-peak-power operation of a Q-switched  $Tm^{3+}$ -doped silica fiber laser operating near  $2 \mu m$ ," *Opt. Lett.* **28**, 22–24 (2003).
- <sup>133</sup>H. Lee and G. Agrawal, "Suppression of stimulated Brillouin scattering in optical fibers using fiber Bragg gratings," *Opt. Express* **11**, 3467–3472 (2003).
- <sup>134</sup>J. M. Chavez Boggio, J. D. Marconi, and H. L. Fragnito, "Experimental and numerical investigation of the SBS-threshold increase in an optical fiber by applying strain distributions," *J. Lightwave Technol.* **23**, 3808–3814 (2005).
- <sup>135</sup>V. I. Kovalev and R. G. Harrison, "Suppression of stimulated Brillouin scattering in high-power single-frequency fiber amplifiers," *Opt. Lett.* **31**, 161–163 (2006).
- <sup>136</sup>A. Liu, "Suppressing stimulated Brillouin scattering in fiber amplifiers using nonuniform fiber and temperature gradient," *Opt. Express* **15**, 977–984 (2007).
- <sup>137</sup>M. Merklein, I. V. Kabakova, T. F. S. Büttner, D.-Y. Choi, B. Luther-Davies, S. J. Madden, and B. J. Eggleton, "Enhancing and inhibiting stimulated Brillouin scattering in photonic integrated circuits," *Nat. Commun.* **6**, 6396 (2015).
- <sup>138</sup>O. Florez, P. F. Jarschel, Y. A. V. Espinel, C. M. B. Cordeiro, T. P. Mayer Alegre, G. S. Wiederhecker, and P. Dainese, "Brillouin scattering self-cancellation," *Nat. Commun.* **7**, 11759 (2016).
- <sup>139</sup>Z. Lou, K. Han, X. Wang, H. Zhang, and X. Xu, "Increasing the SBS threshold by applying a flexible temperature modulation technique with temperature measurement of the fiber core," *Opt. Express* **28**, 13323–13335 (2020).
- <sup>140</sup>A. V. Harish and J. Nilsson, "Optimization of phase modulation formats for suppression of stimulated Brillouin scattering in optical fibers," *IEEE J. Sel. Top. Quantum Electron.* **24**, 5100110 (2018).
- <sup>141</sup>Y. Takushima and T. Okoshi, "Suppression of simulated Brillouin scattering using optical isolators," *Electron. Lett.* **28**, 1155 (1992).
- <sup>142</sup>A. Choudhary, M. Pelusi, D. Marpaung, T. Inoue, K. Vu, P. Ma, D.-Y. Choi, S. Madden, S. Namiki, and B. J. Eggleton, "On-chip Brillouin purification for frequency comb-based coherent optical communications," *Opt. Lett.* **42**, 5074–5077 (2017).
- <sup>143</sup>C. Li, M. Merklein, Y. Liu, A. Choudhary, B. J. Eggleton, and B. Corcoran, "Effective linewidth reduction in self-homodyne coherent reception by stimulated Brillouin scattering-based optical carrier recovery," *Opt. Express* **29**, 25697–25708 (2021).
- <sup>144</sup>E. Giacomidis, A. Choudhary, E. Magi, D. Marpaung, K. Vu, P. Ma, D.-Y. Choi, S. Madden, B. Corcoran, M. Pelusi, and B. J. Eggleton, "Chip-based Brillouin processing for carrier recovery in self-coherent optical communications," *Optica* **5**, 1191 (2018).
- <sup>145</sup>M. Pelusi, T. Inoue, and S. Namiki, "Narrowband and low-noise Brillouin amplification for coherent communications," in *Optical Fiber Communication Conference (OFC)* (Optical Society of America, 2020), p. M11.1.
- <sup>146</sup>M. Pelusi, T. Inoue, and S. Namiki, "Enhanced carrier to noise ratio by Brillouin amplification for optical communications," *J. Lightwave Technol.* **38**, 319–331 (2020).
- <sup>147</sup>M. Pelusi, T. Inoue, and S. Namiki, "Carrier to noise ratio improvement by Brillouin amplification for 64-qam coherent communications," in *Optical Fiber Communication Conference (OFC)* (Optical Society of America, 2019), p. M1B.7.
- <sup>148</sup>A. Zarifi, M. Merklein, Y. Liu, A. Choudhary, B. J. Eggleton, and B. Corcoran, "EDFA-band coverage broadband SBS filter for optical carrier recovery," in *Conference on Lasers and Electro-Optics Pacific Rim (CLEO-PR)* (Optical Society of America, 2020), pp. 1–2.
- <sup>149</sup>T. Kurashima, T. Horiguchi, and M. Tateda, "Distributed-temperature sensing using stimulated Brillouin scattering in optical silica fibers," *Opt. Lett.* **15**, 1038–1040 (1990).
- <sup>150</sup>X. Bao, D. J. Webb, and D. A. Jackson, "32-km distributed temperature sensor based on Brillouin loss in an optical fiber," *Opt. Lett.* **18**, 1561 (1993).
- <sup>151</sup>A. Fellay, L. Thévenaz, M. Facchini, M. Niklès, and P. Robert, "Distributed sensing using stimulated Brillouin scattering: Towards ultimate resolution," in *12th International Conference on Optical Fiber Sensors* (Optical Society of America, Washington, DC, 1997), Vol. 16, p. OWD3.
- <sup>152</sup>A. Brown, B. Colpitts, and K. Brown, "Distributed sensor based on dark-pulse Brillouin scattering," *IEEE Photonics Technol. Lett.* **17**, 1501–1503 (2005).
- <sup>153</sup>A. W. Brown, B. G. Colpitts, and K. Brown, "Dark-pulse Brillouin optical time-domain sensor with 20-mm spatial resolution," *J. Lightwave Technol.* **25**, 381–386 (2007).
- <sup>154</sup>S. M. Foaeng, M. Tur, J.-C. Beugnot, and L. Thevenaz, "High spatial and spectral resolution long-range sensing using Brillouin echoes," *J. Lightwave Technol.* **28**, 2993–3003 (2010).
- <sup>155</sup>T. Hasegawa and K. Hotate, "Measurement of Brillouin gain spectrum distribution along an optical fiber by direct frequency modulation of a laser diode," *Proc. SPIE* **3860**, 306–316 (1999).
- <sup>156</sup>K. Hotate and Z. He, "Synthesis of optical-coherence function and its applications in distributed and multiplexed optical sensing," *J. Lightwave Technol.* **24**, 2541–2557 (2006).
- <sup>157</sup>K. Hotate, K. Abe, and K. Y. Song, "Suppression of signal fluctuation in Brillouin optical correlation domain analysis system using polarization diversity scheme," *IEEE Photonics Technol. Lett.* **18**, 2653–2655 (2006).
- <sup>158</sup>K. Y. Song, K. S. Abedin, K. Hotate, M. G. Herráez, and L. Thévenaz, "Highly efficient Brillouin slow and fast light using  $As_2Se_3$  chalcogenide fiber," *Opt. Express* **14**, 5860–5865 (2006).



- <sup>159</sup>K. Hotate, R. Watanabe, Z. He, and M. Kishi, "Measurement of Brillouin frequency shift distribution in PLC by Brillouin optical correlation domain analysis," *IEICE Tech. Rep.* **112**, 95 (2013).
- <sup>160</sup>R. Cohen, Y. London, Y. Antman, and A. Zadok, "Brillouin optical correlation domain analysis with 4 millimeter resolution based on amplified spontaneous emission," *Opt. Express* **22**, 12070 (2014).
- <sup>161</sup>A. Zarifi, B. Stiller, M. Merklein, N. Li, K. Vu, D.-Y. Choi, P. Ma, S. J. Madden, and B. J. Eggleton, "Highly localized distributed Brillouin scattering response in a photonic integrated circuit," *APL Photonics* **3**, 036101 (2018).
- <sup>162</sup>D. Culverhouse, F. Farahi, C. Pannell, and D. Jackson, "Stimulated Brillouin scattering: A means to realise tunable microwave generator or distributed temperature sensor," *Electron. Lett.* **25**, 915 (1989).
- <sup>163</sup>T. Horiguchi, T. Kurashima, and M. Tateda, "A technique to measure distributed strain in optical fibers," *IEEE Photonics Technol. Lett.* **2**, 352–354 (1990).
- <sup>164</sup>M. Niklès, L. Thévenaz, and P. A. Robert, "Simple distributed fiber sensor based on Brillouin gain spectrum analysis," *Opt. Lett.* **21**, 758 (1996).
- <sup>165</sup>T. Horiguchi, K. Shimizu, T. Kurashima, M. Tateda, and Y. Koyamada, "Development of a distributed sensing technique using Brillouin scattering," *J. Lightwave Technol.* **13**, 1296–1302 (1995).
- <sup>166</sup>T. Kurashima, T. Horiguchi, H. Izumita, S. I. Furukawa, and Y. Koyamada, "Brillouin optical-fiber time domain reflectometry," *IEICE Trans. Commun.* **76**, 382–390 (1993).
- <sup>167</sup>K. Shimizu, T. Horiguchi, Y. Koyamada, and T. Kurashima, "Coherent self-heterodyne Brillouin OTDR for measurement of Brillouin frequency shift distribution in optical fibers," *J. Lightwave Technol.* **12**, 730–736 (1994).
- <sup>168</sup>L. Thévenaz and S. F. Mafang, "Distributed fiber sensing using Brillouin echoes," *Proc. SPIE* **7004**, 70043N (2008).
- <sup>169</sup>X. Bao, A. Brown, M. DeMerchant, and J. Smith, "Characterization of the Brillouin-loss spectrum of single-mode fibers by use of very short (<10-ns) pulses," *Opt. Lett.* **24**, 510 (1999).
- <sup>170</sup>K. Kishida, C.-H. Li, and K. Nishiguchi, "Pulse pre-pump method for cm-order spatial resolution of BOTDA," *Proc. SPIE* **5855**, 559–562 (2005).
- <sup>171</sup>K. Y. Song, S. Chin, N. Primerov, and L. Thévenaz, "Time-domain distributed fiber sensor with 1 cm spatial resolution based on Brillouin dynamic grating," *J. Lightwave Technol.* **28**, 2062–2067 (2010).
- <sup>172</sup>Z. Yang, X. Hong, W. Lin, and J. Wu, "Evaluating and overcoming the impact of second echo in Brillouin echoes distributed sensing," *Opt. Express* **24**, 1543–1558 (2016).
- <sup>173</sup>M. A. Soto and L. Thévenaz, "Modeling and evaluating the performance of Brillouin distributed optical fiber sensors," *Opt. Express* **21**, 31347–31366 (2013).
- <sup>174</sup>A. Motil, A. Bergman, and M. Tur, "State of the art of Brillouin fiber-optic distributed sensing," *Opt. Laser Technol.* **78**, 81–103 (2016).
- <sup>175</sup>Y. Dong, "High-performance distributed Brillouin optical fiber sensing," *Photonic Sens.* **11**, 69–90 (2021).
- <sup>176</sup>Y. Cho, M. Alahbabi, M. Gunning, and T. Newson, "50-km single-ended spontaneous-Brillouin-based distributed-temperature sensor exploiting pulsed Raman amplification," *Opt. Lett.* **28**, 1651–1653 (2003).
- <sup>177</sup>M. A. Soto, G. Bolognini, F. D. Pasquale, and L. Thévenaz, "Simplex-coded BOTDA fiber sensor with 1 m spatial resolution over a 50 km range," *Opt. Lett.* **35**, 259–261 (2010).
- <sup>178</sup>A. Dominguez-Lopez, Z. Yang, M. A. Soto, X. Angulo-Vinuesa, S. Martin-Lopez, L. Thevenaz, and M. Gonzalez-Herreraez, "Novel scanning method for distortion-free BOTDA measurements," *Opt. Express* **24**, 10188–10204 (2016).
- <sup>179</sup>Y. Dong, L. Chen, and X. Bao, "Time-division multiplexing-based BOTDA over 100 km sensing length," *Opt. Lett.* **36**, 277–279 (2011).
- <sup>180</sup>Y. Dong, L. Chen, and X. Bao, "Extending the sensing range of Brillouin optical time-domain analysis combining frequency-division multiplexing and in-line EDFAs," *J. Lightwave Technol.* **30**, 1161–1167 (2011).
- <sup>181</sup>Y. Koyamada, Y. Sakairi, N. Takeuchi, and S. Adachi, "Novel technique to improve spatial resolution in Brillouin optical time-domain reflectometry," *IEEE Photonics Technol. Lett.* **19**, 1910–1912 (2007).
- <sup>182</sup>W. Li, X. Bao, Y. Li, and L. Chen, "Differential pulse-width pair BOTDA for high spatial resolution sensing," *Opt. Express* **16**, 21616–21625 (2008).
- <sup>183</sup>A. Dominguez-Lopez, M. A. Soto, S. Martin-Lopez, L. Thevenaz, and M. Gonzalez-Herreraez, "Resolving 1 million sensing points in an optimized differential time-domain Brillouin sensor," *Opt. Lett.* **42**, 1903–1906 (2017).
- <sup>184</sup>M. A. Soto, P. K. Sahu, G. Bolognini, and F. D. Pasquale, "Brillouin-based distributed temperature sensor employing pulse coding," *IEEE Sens. J.* **8**, 225–226 (2008).
- <sup>185</sup>M. A. Soto, G. Bolognini, and F. D. Pasquale, "Long-range simplex-coded BOTDA sensor over 120 km distance employing optical preamplification," *Opt. Lett.* **36**, 232–234 (2011).
- <sup>186</sup>Y. London, Y. Antman, R. Cohen, N. Kimelfeld, N. Levanon, and A. Zadok, "High-resolution long-range distributed Brillouin analysis using dual-layer phase and amplitude coding," *Opt. Express* **22**, 27144–27158 (2014).
- <sup>187</sup>X. Sun, Z. Yang, X. Hong, S. Zaslowski, S. Wang, M. A. Soto, X. Gao, J. Wu, and L. Thévenaz, "Genetic-optimised aperiodic code for distributed optical fibre sensors," *Nat. Commun.* **11**, 5774 (2020).
- <sup>188</sup>Y. Peled, A. Motil, L. Yaron, and M. Tur, "Slope-assisted fast distributed sensing in optical fibers with arbitrary Brillouin profile," *Opt. Express* **19**, 19845–19854 (2011).
- <sup>189</sup>G. Yang, X. Fan, and Z. He, "Strain dynamic range enlargement of slope-assisted BOTDA by using Brillouin phase-gain ratio," *J. Lightwave Technol.* **35**, 4451–4458 (2017).
- <sup>190</sup>D. Garus, K. Krebber, F. Schliep, and T. Gogolla, "Distributed sensing technique based on Brillouin optical-fiber frequency-domain analysis," *Opt. Lett.* **21**, 1402–1404 (1996).
- <sup>191</sup>R. Bernini, A. Minardo, and L. Zeni, "Distributed Sensing at centimeter-scale spatial resolution by BOFDA: Measurements and signal processing," *IEEE Photonics J.* **4**, 48–56 (2012).
- <sup>192</sup>A. Zadok, Y. Antman, N. Primerov, A. Denisov, J. Sancho, and L. Thevenaz, "Random-access distributed fiber sensing," *Laser Photonics Rev.* **6**, L1–L5 (2012).
- <sup>193</sup>K. Hotate and T. Hasegawa, "Measurement of Brillouin gain spectrum distribution along an optical fiber using a correlation-based technique: Proposal, experiment and simulation," *IEICE Trans. Electron.* **E83**, 405–412 (2000).
- <sup>194</sup>D. Chow, J. C. Tchahame Noughni, A. Denisov, J.-C. Beugnot, T. Sylvestre, L. Li, R. Ahmad, M. Rochette, K. H. Tow, M. A. Soto, and L. Thévenaz, "Mapping the uniformity of optical microwires using phase-correlation Brillouin distributed measurements," in *Frontiers in Optics* (Optical Society of America, Washington, DC, 2015), p. FW4F.4.
- <sup>195</sup>Y. Antman, N. Levanon, and A. Zadok, "Low-noise delays from dynamic Brillouin gratings based on perfect Golomb coding of pump waves," *Opt. Lett.* **37**, 5259–5261 (2012).
- <sup>196</sup>D. Elooz, Y. Antman, N. Levanon, and A. Zadok, "High-resolution long-reach distributed Brillouin sensing based on combined time-domain and correlation-domain analysis," *Opt. Express* **22**, 6453–6463 (2014).
- <sup>197</sup>A. Denisov, M. A. Soto, and L. Thévenaz, "Going beyond 1000000 resolved points in a Brillouin distributed fiber sensor: Theoretical analysis and experimental demonstration," *Light: Sci. Appl.* **5**, e16074 (2016).
- <sup>198</sup>Y. Antman, N. Primerov, J. Sancho, L. Thevenaz, and A. Zadok, "Localized and stationary dynamic gratings via stimulated Brillouin scattering with phase modulated pumps," *Opt. Express* **20**, 7807–7821 (2012).
- <sup>199</sup>K. Y. Song, W. Zou, Z. He, and K. Hotate, "Optical time-domain measurement of Brillouin dynamic grating spectrum in a polarization-maintaining fiber," *Opt. Lett.* **34**, 1381–1383 (2009).
- <sup>200</sup>K. Y. Song, K. Hotate, W. Zou, and Z. He, "Applications of Brillouin dynamic grating to distributed fiber sensors," *J. Lightwave Technol.* **35**, 3268–3280 (2017).
- <sup>201</sup>W. Zou, Z. He, and K. Hotate, "Complete discrimination of strain and temperature using Brillouin frequency shift and birefringence in a polarization-maintaining fiber," *Opt. Express* **17**, 1248–1255 (2009).
- <sup>202</sup>T. R. Parker, M. Farhadiroushan, V. A. Handerek, and a J. Rogers, "Temperature and strain dependence of the power level and frequency of spontaneous Brillouin scattering in optical fibers," *Opt. Lett.* **22**, 787–789 (1997).
- <sup>203</sup>R. M. Shelby, M. D. Levenson, and P. W. Bayer, "Guided acoustic-wave Brillouin scattering," *Phys. Rev. B* **31**, 5244–5252 (1985).
- <sup>204</sup>G. Bashan, H. H. Diamandi, Y. London, E. Preter, and A. Zadok, "Optomechanical time-domain reflectometry," *Nat. Commun.* **9**, 2991 (2018).
- <sup>205</sup>D. M. Chow, Z. Yang, M. A. Soto, and L. Thévenaz, "Distributed forward Brillouin sensor based on local light phase recovery," *Nat. Commun.* **9**, 2990 (2018).

- <sup>206</sup>T. G. Euser, J. S. Y. Chen, M. Scharrer, P. S. J. Russell, N. J. Farrer, and P. J. Sadler, "Quantitative broadband chemical sensing in air-suspended solid-core fibers," *J. Appl. Phys.* **103**, 103108 (2008).
- <sup>207</sup>I. Dicaire, A. De Rossi, S. Combré, and L. Thévenaz, "Probing molecular absorption under slow-light propagation using a photonic crystal waveguide," *Opt. Lett.* **37**, 4934 (2012).
- <sup>208</sup>T. Ritari, J. Tuominen, and H. Ludvigsen, "Gas sensing using air-guiding photonic bandgap fibers," *Opt. Express* **12**, 4080 (2004).
- <sup>209</sup>D. K. C. Wu, B. T. Kuhlmeiy, and B. J. Eggleton, "Ultrasensitive photonic crystal fiber refractive index sensor," *Opt. Lett.* **34**, 322 (2009).
- <sup>210</sup>S. Zaslawski, Z. Yang, S. Wang, and L. Thévenaz, "Distributed forward stimulated Brillouin scattering measurement using broadband BOTDR," *Proc. SPIE* **11199**, 323–326 (2019).
- <sup>211</sup>C. Pang, Z. Hua, D. Zhou, H. Zhang, L. Chen, X. Bao, and Y. Dong, "Optomechanical time-domain analysis based on coherent forward stimulated Brillouin scattering probing," *Optica* **7**, 176–184 (2020).
- <sup>212</sup>S. Zaslawski, Z. Yang, and L. Thévenaz, "Distributed optomechanical fiber sensing based on serrodyne analysis," *Optica* **8**, 388–395 (2021).
- <sup>213</sup>H. H. Diamandi, Y. London, G. Bashan, K. Shemer, and A. Zadok, "Forward stimulated Brillouin scattering analysis of optical fibers coatings," *J. Lightwave Technol.* **39**, 1800–1807 (2021).
- <sup>214</sup>K. Sharma, E. Zehavi, H. H. Diamandi, G. Bashan, Y. London, and A. Zadok, "Direct time-of-flight distributed analysis of nonlinear forward scattering," *Optica* **9**, 419–428 (2022).
- <sup>215</sup>J. Song, X. Guo, W. Peng, J. Pan, L. Wan, T. Feng, S. Zeng, D. Liu, B. Zhang, M. Zhang, and Z. Li, "Stimulated Brillouin scattering in low-loss  $\text{Ge}_{25}\text{Sb}_{10}\text{S}_{65}$  chalcogenide waveguides," *J. Lightwave Technol.* **39**, 5048–5053 (2021).
- <sup>216</sup>B. Morrison, A. Casas-Bedoya, G. Ren, K. Vu, Y. Liu, A. Zarifi, T. G. Nguyen, D.-Y. Choi, D. Marpaung, S. J. Madden, A. Mitchell, and B. J. Eggleton, "Compact Brillouin devices through hybrid integration on silicon," *Optica* **4**, 847 (2017).
- <sup>217</sup>C. K. Lai, D. Y. Choi, N. J. Athanasios, K. Yan, W. Y. Chong, S. Debbarma, H. Ahmad, B. J. Eggleton, M. Merklein, and S. J. Madden, "Hybrid chalcogenide-germanosilicate waveguides for high performance stimulated Brillouin scattering applications," *Adv. Funct. Mater.* **32**, 2105230 (2021).
- <sup>218</sup>T. J. Kippenberg and K. J. Vahala, "Cavity optomechanics: Back-action at the mesoscale," *Science* **321**, 1172–1176 (2008).
- <sup>219</sup>S. Gröblacher, K. Hammerer, M. R. Vanner, and M. Aspelmeyer, "Observation of strong coupling between a micromechanical resonator and an optical cavity field," *Nature* **460**, 724–727 (2009).
- <sup>220</sup>G. S. Wiederhecker, L. Chen, A. Gondarenko, and M. Lipson, "Controlling photonic structures using optical forces," *Nature* **462**, 633–636 (2009).
- <sup>221</sup>S. Weis, R. Riviere, S. Deleglise, E. Gavartin, O. Arcizet, A. Schliesser, and T. J. Kippenberg, "Optomechanically induced transparency," *Science* **330**, 1520–1523 (2010).
- <sup>222</sup>J. Chan, T. P. M. Alegre, A. H. Safavi-Naeini, J. T. Hill, A. Krause, S. Gröblacher, M. Aspelmeyer, and O. Painter, "Laser cooling of a nanomechanical oscillator into its quantum ground state," *Nature* **478**, 89–92 (2011).
- <sup>223</sup>J. D. Teufel, D. Li, M. S. Allman, K. Cicak, A. J. Sirois, J. D. Whittaker, and R. W. Simmonds, "Circuit cavity electromechanics in the strong-coupling regime," *Nature* **471**, 204–208 (2011).
- <sup>224</sup>A. H. Safavi-Naeini, T. P. Mayer Alegre, J. Chan, M. Eichenfeld, M. Winger, Q. Lin, J. T. Hill, D. E. Chang, and O. Painter, "Electromagnetically induced transparency and slow light with optomechanics," *Nature* **472**, 69–73 (2011).
- <sup>225</sup>D. W. C. Brooks, T. Botter, S. Schreppler, T. P. Purdy, N. Brahm, and D. M. Stamper-Kurn, "Non-classical light generated by quantum-noise-driven cavity optomechanics," *Nature* **488**, 476–480 (2012), 1107.5609.
- <sup>226</sup>A. H. Safavi-Naeini, J. Chan, J. T. Hill, T. P. M. Alegre, A. Krause, and O. Painter, "Observation of quantum motion of a nanomechanical resonator," *Phys. Rev. Lett.* **108**, 033602 (2012).
- <sup>227</sup>E. Verhagen, S. Deléglise, S. Weis, A. Schliesser, and T. J. Kippenberg, "Quantum-coherent coupling of a mechanical oscillator to an optical cavity mode," *Nature* **482**, 63–67 (2012).
- <sup>228</sup>C. Dong, V. Fiore, M. C. Kuzyk, and H. Wang, "Optomechanical dark mode," *Science* **338**, 1609–1613 (2012).
- <sup>229</sup>T. A. Palomaki, J. W. Harlow, J. D. Teufel, R. W. Simmonds, and K. W. Lehnert, "Coherent state transfer between itinerant microwave fields and a mechanical oscillator," *Nature* **495**, 210–214 (2013).
- <sup>230</sup>R. Riedinger, S. Hong, R. A. Norte, J. A. Slater, J. Shang, A. G. Krause, V. Anant, M. Aspelmeyer, and S. Gröblacher, "Non-classical correlations between single photons and phonons from a mechanical oscillator," *Nature* **530**, 313–316 (2016).
- <sup>231</sup>Y. Chu, P. Kharel, W. H. Renninger, L. D. Burkhardt, L. Frunzio, P. T. Rakich, and R. J. Schoelkopf, "Quantum acoustics with superconducting qubits," *Science* **358**, 199–202 (2017).
- <sup>232</sup>A. H. Safavi-Naeini, D. Van Thourhout, R. Baets, and R. Van Laer, "Controlling phonons and photons at the wavelength scale: Integrated photonics meets integrated phononics," *Optica* **6**, 213 (2019).
- <sup>233</sup>C. G. Poulton, R. Pant, and B. J. Eggleton, "Acoustic confinement and stimulated Brillouin scattering in integrated optical waveguides," *J. Opt. Soc. Am. B* **30**, 2657–2664 (2013).
- <sup>234</sup>P. T. Rakich, C. Reinke, R. Camacho, P. Davids, and Z. Wang, "Giant enhancement of stimulated Brillouin scattering in the subwavelength limit," *Phys. Rev. X* **2**, 011008 (2012).
- <sup>235</sup>J. C. Knight, T. A. Birks, P. S. J. Russell, and D. Atkin, "All-silica signal-mode optical fiber with photonic crystal cladding," *Opt. Lett.* **21**, 1547–1549 (1996).
- <sup>236</sup>P. S. J. Russell, "Photonic crystal fibers," *Science* **299**, 358–362 (2003).
- <sup>237</sup>P. Dainese, P. S. J. Russell, N. Joly, J. C. Knight, G. S. Wiederhecker, H. L. Fragnito, V. Laude, and A. Khelif, "Stimulated Brillouin scattering from multi-GHz-guided acoustic phonons in nanostructured photonic crystal fibres," *Nat. Phys.* **2**, 388 (2006).
- <sup>238</sup>J. R. Sandercock, "Structure in the Brillouin spectra of thin films," *Phys. Rev. Lett.* **29**, 1735–1738 (1972).
- <sup>239</sup>N. Rowell, V. C. Y. So, and G. I. Stegeman, "Brillouin scattering in a thin-film waveguide," *Appl. Phys. Lett.* **32**, 154–155 (1978).
- <sup>240</sup>N. L. Rowell, P. J. Thomas, H. M. Van Driel, and G. I. Stegeman, "Brillouin spectrum of single-mode optical fibers," *Appl. Phys. Lett.* **34**, 139–141 (1979).
- <sup>241</sup>N. L. Rowell and G. I. Stegeman, "Brillouin scattering from surface phonons in thin films," *Phys. Rev. Lett.* **41**, 970–973 (1978).
- <sup>242</sup>R. Loudon, "Theory of surface-ripple Brillouin scattering by solids," *Phys. Rev. Lett.* **40**, 581–583 (1978).
- <sup>243</sup>R. Normandin, V. C.-Y. So, N. Rowell, and G. I. Stegeman, "Scattering of guided optical beams by surface acoustic waves in thin films," *J. Opt. Soc. Am.* **69**, 1153 (1979).
- <sup>244</sup>D. Elser, U. L. Andersen, A. Korn, O. Glöckl, S. Lorenz, C. Marquardt, and G. Leuchs, "Reduction of guided acoustic wave Brillouin scattering in photonic crystal fibers," *Phys. Rev. Lett.* **97**(13), 133901 (2006).
- <sup>245</sup>J.-C. Beugnot, T. Sylvestre, H. Maillotte, G. Mélin, and V. Laude, "Guided acoustic wave Brillouin scattering in photonic crystal fibers," *Opt. Lett.* **32**, 17 (2007).
- <sup>246</sup>D. Elser, C. Wittmann, U. L. Andersen, O. Glöckl, S. Lorenz, C. Marquardt, and G. Leuchs, "Guided acoustic wave Brillouin scattering in photonic crystal fibers," *J. Phys.: Conf. Ser.* **92**, 012108 (2007).
- <sup>247</sup>B. Stiller, M. Delqué, J.-C. Beugnot, M. W. Lee, G. Mélin, H. Maillotte, V. Laude, and T. Sylvestre, "Frequency-selective excitation of guided acoustic modes in a photonic crystal fiber," *Opt. Express* **19**, 7689 (2011).
- <sup>248</sup>V. Laude and J. C. Beugnot, "Generation of phonons from electrostriction in small-core optical waveguides," *AIP Adv.* **3**, 042109 (2013).
- <sup>249</sup>I. Aryanfar, D. Marpaung, A. Choudhary, Y. Liu, K. Vu, D.-Y. Choi, P. Ma, S. Madden, and B. J. Eggleton, "Chip-based Brillouin radio frequency photonic phase shifter and wideband time delay," *Opt. Lett.* **42**, 1313 (2017).
- <sup>250</sup>A. Choudhary, B. Morrison, I. Aryanfar, S. Shahnia, M. Pagani, Y. Liu, K. Vu, S. Madden, D. Marpaung, and B. J. Eggleton, "Advanced integrated microwave signal processing with giant on-chip Brillouin gain," *J. Lightwave Technol.* **35**, 846–854 (2017).
- <sup>251</sup>S. Levy, V. Lyubin, M. Klebanov, J. Scheuer, and A. Zadok, "Stimulated Brillouin scattering amplification in centimeter-long directly written chalcogenide waveguides," *Opt. Lett.* **37**, 5112–5114 (2012).
- <sup>252</sup>T. F. S. Büttner, M. Merklein, I. V. Kabakova, D. D. Hudson, D.-Y. Choi, B. Luther-Davies, S. J. Madden, and B. J. Eggleton, "Phase-locked, chip-based, cascaded stimulated Brillouin scattering," *Optica* **1**, 311 (2014).
- <sup>253</sup>E. A. Kittlaus, H. Shin, and P. T. Rakich, "Large Brillouin amplification in silicon," *Nat. Photonics* **10**, 463–467 (2016).
- <sup>254</sup>H. Shin, J. A. Cox, R. Jarecki, A. Starbuck, Z. Wang, and P. T. Rakich, "Control of coherent information via on-chip photonic-phononic emitter-receivers," *Nat. Commun.* **6**, 6427 (2015).

- <sup>255</sup>H. Shin, W. Qiu, R. Jarecki, J. A. Cox, R. H. Olsson, A. Starbuck, Z. Wang, and P. T. Rakich, "Tailorable stimulated Brillouin scattering in nanoscale silicon waveguides," *Nat. Commun.* **4**, 1944 (2013).
- <sup>256</sup>E. A. Kittlaus, N. T. Otterstrom, and P. T. Rakich, "On-chip inter-modal Brillouin scattering," *Nat. Commun.* **8**, 15819 (2017).
- <sup>257</sup>C. Wolff, P. Gutsche, M. J. Steel, B. J. Eggleton, and C. G. Poulton, "Impact of nonlinear loss on stimulated Brillouin scattering," *J. Opt. Soc. Am. B* **32**, 1968 (2015).
- <sup>258</sup>R. V. Laer, A. Bazin, B. Kuyken, R. Baets, and D. V. Thourhout, "Net on-chip Brillouin gain based on suspended silicon nanowires," *New J. Phys.* **17**, 115005 (2015).
- <sup>259</sup>C. Wolff, P. Gutsche, M. J. Steel, B. J. Eggleton, and C. G. Poulton, "Power limits and a figure of merit for stimulated Brillouin scattering in the presence of third and fifth order loss," *Opt. Express* **23**, 26628 (2015).
- <sup>260</sup>Y. H. Lai, M. G. Suh, Y. K. Lu, B. Shen, Q. F. Yang, H. Wang, J. Li, S. H. Lee, K. Y. Yang, and K. Vahala, "Earth rotation measured by a chip-scale ring laser gyroscope," *Nat. Photonics* **14**, 345 (2020).
- <sup>261</sup>K. Y. Yang, D. Y. Oh, S. H. Lee, Q. F. Yang, X. Yi, B. Shen, H. Wang, and K. Vahala, "Bridging ultrahigh-Q devices and photonic circuits," *Nat. Photonics* **12**, 297–302 (2018).
- <sup>262</sup>S. Gundavarapu, G. M. Brodnik, M. Puckett, T. Huffman, D. Bose, R. Behunin, J. Wu, T. Qiu, C. Pinho, N. Chauhan, J. Nohava, P. T. Rakich, K. D. Nelson, M. Salit, and D. J. Blumenthal, "Sub-hertz fundamental linewidth photonic integrated Brillouin laser," *Nat. Photonics* **13**, 60 (2018).
- <sup>263</sup>D. G. Kim, S. Han, J. Hwang, I. H. Do, D. Jeong, J. H. Lim, Y. H. Lee, M. Choi, Y. H. Lee, D. Y. Choi, and H. Lee, "Universal light-guiding geometry for on-chip resonators having extremely high Q-factor," *Nat. Commun.* **11**, 5933 (2020).
- <sup>264</sup>N. T. Otterstrom, E. A. Kittlaus, S. Gertler, R. O. Behunin, A. L. Lentine, and P. T. Rakich, "Resonantly enhanced nonreciprocal silicon Brillouin amplifier," *Optica* **6**, 1117 (2019), 1903.03907.
- <sup>265</sup>N. T. Otterstrom, R. O. Behunin, E. A. Kittlaus, Z. Wang, and P. T. Rakich, "A silicon Brillouin laser," *Science* **360**, 1113–1116 (2018).
- <sup>266</sup>F. G. S. Santos, Y. A. V. Espinel, G. O. Luiz, R. S. Benevides, G. S. Wiederhecker, and T. P. Mayer Alegre, "Hybrid confinement of optical and mechanical modes in a bullseye optomechanical resonator," *Opt. Express* **25**, 508 (2017).
- <sup>267</sup>E. A. Kittlaus, N. T. Otterstrom, P. Kharel, S. Gertler, and P. T. Rakich, "Non-reciprocal interband Brillouin modulation," *Nat. Photonics* **12**, 613–620 (2018).
- <sup>268</sup>S. Gertler, E. A. Kittlaus, N. T. Otterstrom, and P. T. Rakich, "Tunable microwave-photonic filtering with high out-of-band rejection in silicon," *APL Photonics* **5**, 096103 (2020).
- <sup>269</sup>M. Tomes and T. Carmon, "Photonic micro-electromechanical systems vibrating at X-band (11-GHz) rates," *Phys. Rev. Lett.* **102**, 113601 (2009).
- <sup>270</sup>H. Lee, T. Chen, J. Li, K. Y. Yang, S. Jeon, O. Painter, and K. J. Vahala, "Chemically etched ultrahigh-Q wedge-resonator on a silicon chip," *Nat. Photonics* **6**, 369–373 (2012).
- <sup>271</sup>F. Gyger, J. Liu, F. Yang, J. He, A. S. Raja, R. N. Wang, S. A. Bhave, T. J. Kippenberg, and L. Thévenaz, "Observation of stimulated Brillouin scattering in silicon nitride integrated waveguides," *Phys. Rev. Lett.* **124**, 013902 (2020).
- <sup>272</sup>R. Botter, K. Ye, Y. Klaver, R. Suryadharma, O. Daulay, G. Liu, J. van den Hoogen, L. Kanger, P. van der Slot, E. Klein, M. Hoekman, C. Roeloffzen, Y. Liu, and D. Marpaung, "Guided-acoustic stimulated Brillouin scattering in silicon nitride photonic circuits," *Sci. Adv.* **8**, eabq2196 (2022).
- <sup>273</sup>W. Jin, L. Chang, W. Xie, H. Shu, J. D. Peters, X. Wang, and J. E. Bowers, "Stimulated Brillouin scattering in AlGaAs on insulator waveguides," in *Conference on Lasers and Electro-Optics* (Optical Society of America, Washington, DC, 2020), Vol. 11, p. SM4L.7.
- <sup>274</sup>D. B. Sohn, S. Kim, and G. Bahl, "Time-reversal symmetry breaking with acoustic pumping of nanophotonic circuits," *Nat. Photonics* **12**, 91–97 (2018).
- <sup>275</sup>E. A. Kittlaus, W. M. Jones, P. T. Rakich, N. T. Otterstrom, R. E. Muller, and M. Rais-Zadeh, "Electrically driven acousto-optics and broadband non-reciprocity in silicon photonics," *Nat. Photonics* **15**, 43–52 (2021).
- <sup>276</sup>Q. Liu, H. Li, and M. Li, "Electromechanical Brillouin scattering in integrated optomechanical waveguides," *Optica* **6**, 778 (2019).
- <sup>277</sup>R. Van Laer, R. N. Patel, T. P. McKenna, J. D. Witmer, and A. H. Safavi-Naeini, "Electrical driving of X-band mechanical waves in a silicon photonic circuit," *APL Photonics* **3**, 086102 (2018).
- <sup>278</sup>D. Munk, M. Katzman, M. Hen, M. Priel, M. Feldberg, T. Sharabani, S. Levy, A. Bergman, and A. Zadok, "Surface acoustic wave photonic devices in silicon on insulator," *Nat. Commun.* **10**, 4214 (2019).
- <sup>279</sup>B. J. Eggleton, C. G. Poulton, and R. Pant, "Inducing and harnessing stimulated Brillouin scattering in photonic integrated circuits," *Adv. Opt. Photonics* **5**, 536–587 (2013).
- <sup>280</sup>M. Merklein, B. Stiller, and B. J. Eggleton, "Brillouin-based light storage and delay techniques," *J. Opt.* **20**, 083003 (2018).
- <sup>281</sup>D. Marpaung, J. Yao, and J. Capmany, "Integrated microwave photonics," *Nat. Photonics* **13**, 80 (2019).
- <sup>282</sup>D. Marpaung, B. Morrison, M. Pagani, R. Pant, D.-Y. Choi, B. Luther-Davies, S. J. Madden, and B. J. Eggleton, "Low-power, chip-based stimulated Brillouin scattering microwave photonic filter with ultrahigh selectivity," *Optica* **2**, 76 (2015).
- <sup>283</sup>H. Jiang, D. Marpaung, M. Pagani, K. Vu, D.-Y. Choi, S. J. Madden, L. Yan, and B. J. Eggleton, "Wide-range, high-precision multiple microwave frequency measurement using a chip-based photonic Brillouin filter," *Optica* **3**, 30 (2016).
- <sup>284</sup>Z. Zhu, D.-Y. Choi, S. J. Madden, B. J. Eggleton, and M. Merklein, "High-conversion-gain and deep-image-rejection Brillouin chip-based photonic RF mixer," *Opt. Lett.* **45**, 5571 (2020).
- <sup>285</sup>J. Li, H. Lee, and K. J. Vahala, "Microwave synthesizer using an on-chip Brillouin oscillator," *Nat. Commun.* **4**, 2097 (2013).
- <sup>286</sup>L. McKay, M. Merklein, A. C. Bedoya, A. Choudhary, M. Jenkins, C. Middleton, A. Cramer, J. Devenport, A. Klee, R. DeSalvo, and B. J. Eggleton, "Brillouin-based phase shifter in a silicon waveguide," *Optica* **6**, 907 (2019).
- <sup>287</sup>A. Byrnes, R. Pant, E. Li, D.-Y. Choi, C. G. Poulton, S. Fan, S. Madden, B. Luther-Davies, and B. J. Eggleton, "Photonic chip based tunable and reconfigurable narrowband microwave photonic filter using stimulated Brillouin scattering," *Opt. Express* **20**, 18836 (2012).
- <sup>288</sup>Y. Liu, A. Choudhary, D. Marpaung, and B. J. Eggleton, "Integrated microwave photonic filters," *Adv. Opt. Photonics* **12**, 485 (2020).
- <sup>289</sup>A. Casas-Bedoya, B. Morrison, M. Pagani, D. Marpaung, and B. J. Eggleton, "Tunable narrowband microwave photonic filter created by stimulated Brillouin scattering from a silicon nanowire," *Opt. Lett.* **40**, 4154 (2015).
- <sup>290</sup>M. Merklein, B. Stiller, I. V. Kabakova, U. S. Mutugala, K. Vu, S. J. Madden, B. J. Eggleton, and R. Slavik, "Widely tunable, low phase noise microwave source based on a photonic chip," *Opt. Lett.* **41**, 4633 (2016).
- <sup>291</sup>Z. Zhu, M. Merklein, D.-Y. Choi, K. Vu, P. Ma, S. J. Madden, and B. J. Eggleton, "Highly sensitive, broadband microwave frequency identification using a chip-based Brillouin optoelectronic oscillator," *Opt. Express* **27**, 12855 (2019).
- <sup>292</sup>M. Garrett, M. Merklein, and B. J. Eggleton, "Chip-based Brillouin processing for microwave photonic phased array antennas," *IEEE J. Sel. Top. Quantum Electron.* **2022**, 1–21.
- <sup>293</sup>M. Pagani, D. Marpaung, D.-Y. Choi, S. J. Madden, B. Luther-Davies, and B. Eggleton, "Tunable wideband microwave photonic phase shifter using on-chip stimulated Brillouin scattering," *Opt. Express* **22**, 28810–28818 (2014).
- <sup>294</sup>P. A. Morton and J. B. Khurgin, "Microwave photonic delay line with separate tuning of the optical carrier," *IEEE Photonics Technol. Lett.* **21**, 1686–1688 (2009).
- <sup>295</sup>L. McKay, M. Merklein, A. Choudhary, Y. Liu, M. Jenkins, C. Middleton, A. Cramer, A. Chilton, J. Devenport, K. Vu, D. Y. Choi, P. Ma, S. J. Madden, R. DeSalvo, and B. J. Eggleton, "Broadband Brillouin phase shifter utilizing RF interference: Experimental demonstration and theoretical analysis," *J. Lightwave Technol.* **38**, 3624–3636 (2020).
- <sup>296</sup>L. McKay, M. Merklein, Y. Liu, A. Cramer, J. Maksymow, A. Chilton, K. Yan, D.-Y. Choi, S. J. Madden, R. DeSalvo, and B. J. Eggleton, "Integrated microwave photonic true-time delay with interferometric delay enhancement based on Brillouin scattering and microring resonators," *Opt. Express* **28**, 36020 (2020).
- <sup>297</sup>A. Zariifi, B. Stiller, M. Merklein, Y. Liu, B. Morrison, A. Casas-Bedoya, G. Ren, T. G. Nguyen, K. Vu, D.-Y. Choi, A. Mitchell, S. J. Madden, and B. J.

- Eggleton, "Brillouin spectroscopy of a hybrid silicon-chalcogenide waveguide with geometrical variations," *Opt. Lett.* **43**, 3493 (2018).
- <sup>298</sup>A. Zarifi, B. Stiller, M. Merklein, Y. Liu, B. Morrison, A. Casas-Bedoya, G. Ren, T. G. Nguyen, K. Vu, D.-Y. Choi, A. Mitchell, S. J. Madden, and B. J. Eggleton, "On-chip correlation-based Brillouin sensing: Design, experiment, and simulation," *J. Opt. Soc. Am. B* **36**, 146 (2019).
- <sup>299</sup>H. Li, Q. Liu, and M. Li, "Electromechanical Brillouin scattering in integrated planar photonics," *APL Photonics* **4**, 080802 (2019).
- <sup>300</sup>M. Merklein, B. Stiller, K. Vu, S. J. Madden, and B. J. Eggleton, "A chip-integrated coherent photonic-phononic memory," *Nat. Commun.* **8**, 574 (2017).
- <sup>301</sup>J. Li, H. Lee, T. Chen, and K. J. Vahala, "Characterization of a high coherence, Brillouin microcavity laser on silicon," *Opt. Express* **20**, 20170 (2012).
- <sup>302</sup>M. G. Suh, Q. F. Yang, and K. J. Vahala, "Phonon-limited-linewidth of Brillouin lasers at cryogenic temperatures," *Phys. Rev. Lett.* **119**, 143901 (2017).
- <sup>303</sup>N. Chauhan, A. Isichenko, K. Liu, J. Wang, Q. Zhao, R. O. Behunin, P. T. Rakich, A. M. Jayich, C. Fertig, C. W. Hoyt, and D. J. Blumenthal, "Visible light photonic integrated Brillouin laser," *Nat. Commun.* **12**, 4685 (2021).
- <sup>304</sup>X. Huang and S. Fan, "Complete all-optical silica fiber isolator via stimulated Brillouin scattering," *J. Lightwave Technol.* **29**, 2267–2275 (2011).
- <sup>305</sup>R. Pant, A. Byrnes, C. G. Poulton, E. Li, D.-Y. Choi, S. Madden, B. Luther-Davies, and B. J. Eggleton, "Photonic-chip-based tunable slow and fast light via stimulated Brillouin scattering," *Opt. Lett.* **37**, 969 (2012).
- <sup>306</sup>K. Jaksch, M. Merklein, K. Vu, P. Ma, S. J. Madden, B. J. Eggleton, and B. Stiller, "Brillouin-based light storage of 200ps-long pulses for 70 pulse widths," in *Frontiers in Optics* (Optical Society of America, Washington, DC, 2017), p. FTh4A.5.
- <sup>307</sup>B. Stiller, M. Merklein, C. Wolff, K. Vu, P. Ma, S. J. Madden, and B. J. Eggleton, "Coherently refreshing hypersonic phonons for light storage," *Optica* **7**, 492 (2020).
- <sup>308</sup>B. Stiller, M. Merklein, K. Vu, P. Ma, S. J. Madden, C. G. Poulton, and B. J. Eggleton, "Cross talk-free coherent multi-wavelength Brillouin interaction," *APL Photonics* **4**, 040802 (2019).
- <sup>309</sup>M. Merklein, B. Stiller, K. Vu, P. Ma, S. J. Madden, and B. J. Eggleton, "On-chip broadband nonreciprocal light storage," *Nanophotonics* **10**, 75–82 (2021).
- <sup>310</sup>M. K. Schmidt, M. C. O'Brien, M. J. Steel, and C. G. Poulton, "ARRAW: Anti-resonant reflecting acoustic waveguides," *New J. Phys.* **22**, 053011 (2020).
- <sup>311</sup>C. J. Sarabalis, J. T. Hill, and A. H. Safavi-Naeini, "Guided acoustic and optical waves in silicon-on-insulator for Brillouin scattering and optomechanics," *APL Photonics* **1**, 071301 (2016).
- <sup>312</sup>I. V. Kabakova, Y. Xiang, C. Paterson, and P. Török, "Fiber-integrated Brillouin microspectroscopy: Towards Brillouin endoscopy," *J. Innovative Opt. Health Sci.* **10**(6), 1742002 (2017).
- <sup>313</sup>Y. Xiang, C. Basirun, J. Chou, M. E. Warkiani, P. Török, Y. Wang, S. Gao, and I. V. Kabakova, "Background-free fibre optic Brillouin probe for remote mapping of micromechanics," *Biomed. Opt. Express* **11**, 6687–6698 (2020).
- <sup>314</sup>F. Yang, F. Gyger, A. Godet, J. Chrétien, L. Zhang, M. Pang, J.-C. Beugnot, and L. Thévenaz, "Large evanescently-induced Brillouin scattering at the surrounding of a nanofibre," *Nat. Commun.* **13**, 1432 (2022).
- <sup>315</sup>X. Zeng, W. He, M. H. Frosz, A. Geilen, P. Roth, G. K. L. Wong, P. S. Russell, and B. Stiller, "Stimulated Brillouin scattering in chiral photonic crystal fiber," *Photonics Res.* **10**, 711 (2022).
- <sup>316</sup>A. Geilen, A. Popp, D. Walter, M. Chemnitz, S. Junaid, C. G. Poulton, C. Marquardt, M. A. Schmidt, and B. Stiller, "Strong optoacoustic interaction in hot CS<sub>2</sub>-filled liquid-core optical fiber," *Opt. InfoBase Conf. Papers* **25**, 22946 (2021).
- <sup>317</sup>G. Enzian, M. Szczykulska, J. Silver, L. Del Bino, S. Zhang, I. A. Walmsley, P. Del'Haye, and M. R. Vanner, "Observation of Brillouin optomechanical strong coupling with an 11 GHz mechanical mode," *Optica* **6**, 7 (2019).
- <sup>318</sup>X. He, G. I. Harris, C. G. Baker, A. Sawadsky, Y. L. Sfindla, Y. P. Sachkou, S. Forstner, and W. P. Bowen, "Strong optical coupling through superfluid Brillouin lasing," *Nat. Phys.* **16**, 417–421 (2020).
- <sup>319</sup>A. Bergman, R. Duggan, K. Sharma, M. Tur, A. Zadok, and A. Alù, "Observation of anti-parity-time-symmetry, phase transitions and exceptional points in an optical fibre," *Nat. Commun.* **12**, 486 (2021).